Preprint typeset in JHEP style - HYPER VERSION

arXiv:1006.0470 [hep-ph]
IFIC/10-06
FTUV/10-0602

Charged-Higgs phenomenology in the Aligned two-Higgs-doublet model

Martin Jung, Antonio Pich, Paula Tuzón

Instituto de Física Corpuscular (IFIC),CSIC-Universitat de València
Apartado de Correos 22085,E-46071 Valencia, Spain
E-Mail: jung@ific.uv.es
E-Mail: pich@ific.uv.es
E-Mail: tuzon@ific.uv.es

Abstract: The alignment in flavour space of the Yukawa matrices of a general two-Higgs-doublet model results in the absence of tree-level flavour-changing neutral currents. In addition to the usual fermion masses and mixings, the aligned Yukawa structure only contains three complex parameters ς_f, which are potential new sources of CP violation [1]. For particular values of these three parameters all known specific implementations of the model based on discrete $\mathcal{Z}_2$ symmetries are recovered. One of the most distinctive features of the two-Higgs-doublet model is the presence of a charged scalar $H^\pm$. In this work, we discuss its main phenomenological consequences in flavour-changing processes at low energies and derive the corresponding constraints on the parameters of the aligned two-Higgs-doublet model.

Keywords: Beyond Standard Model, CP violation, Higgs Physics.

Contents

1. Introduction

The simplicity of the idea of including one additional Higgs doublet to the Standard Model (SM) and the versatility of the resulting phenomenology are the main ingredients that have made the two-Higgs-doublet model (2HDM, see e.g. [2, 3] and references therein) so interesting. In the most general version of the model, the fermionic couplings of the neutral scalars are non-diagonal in flavour and, therefore, generate unwanted flavour-changing neutral-current (FCNC) phenomena. Different ways to suppress FCNCs have been developed, giving rise to a variety of specific implementations of the 2HDM. The simplest and

most common approach is to impose a $\mathcal{Z}_2$ symmetry forbidding all non-diagonal terms in the Lagrangian [4]. Depending on the charge assignments under this symmetry, the model is called type I [5, 6], II [6, 7], X and Y [8, 9, 10, 11, 12, 13, 14] or *inert* [15, 16, 17, 18]. In these types of models with *natural flavour conservation* the Cabibbo-Kobayashi-Maskawa (CKM) quark mixing matrix [19, 20] is the only possible source of CP violation. Another possibility is to assume particular Yukawa textures which force the non-diagonal Yukawa couplings to be proportional to the geometric mean of the two fermion masses, $g_{ij} \propto \sqrt{m_i m_j}$, the so-called type III 2HDM [21, 22, 23, 24].

Our work focuses on the recent suggestion [1] to enforce the alignment in flavour space of the Yukawa couplings of the two scalar doublets, which guarantees the absence of tree-level FCNC interactions. The Yukawa structure of the resulting aligned two-Higgs-doublet model (A2HDM) is fully characterized by the fermion masses, the CKM quark mixing matrix and three complex parameters ς_f $(f = u, d, l)$, whose phases are potential new sources of CP violation [1]. The usual models based on $\mathcal{Z}_2$ symmetries are recovered for particular (real) values of these three parameters. The A2HDM provides a more general setting to discuss the phenomenology of 2HDMs without tree-level FCNCs, leaving open the possibility of having additional CP-violating phases in the Yukawa sector beyond the CKM-matrix one.

The presence of a charged scalar $H^\pm$ is one of the most distinctive features of an extended scalar sector. In the following we analyze its phenomenological impact in low-energy flavour-changing processes within the A2HDM, and constrain the three complex parameters ς_f with present data on different leptonic, semileptonic and hadronic decays. We proceed as follows: the formulation of the general 2HDM is recalled in section 2, where the *aligned* condition is implemented and the resulting Yukawa structure discussed. Section 3 explains our statistical treatment of theoretical uncertainties and compiles the inputs used in our analysis. The phenomenological consequences of having a charged scalar field are analyzed next, process by process, extracting the corresponding constraints on the new-physics parameters ς_f. In section 4 we discuss the constraints derived from tree-level leptonic and semileptonic decays, while section 5 describes the information obtained from loop-induced processes. Finally, we give our conclusions in section 6. Some technical aspects related to $\Delta F = 2$ transitions have been relegated to the appendix.

2. Aligned two-Higgs-doublet model

The 2HDM extends the SM with a second Higgs doublet of hypercharge $Y = \frac{1}{2}$. The neutral components of the scalar doublets $\phi_a(x)$ $(a = 1, 2)$ acquire vacuum expectation values (VEVs) that are, in general, complex: $\langle 0|\phi_a^T(x)|0\rangle = \frac{1}{\sqrt{2}}\,(0, v_a\, e^{i\theta_a})$. Through an appropriate $U(1)_Y$ transformation we can enforce $\theta_1 = 0$, since only the relative phase $\theta \equiv \theta_2 - \theta_1$ is observable. The combination $v \equiv \sqrt{v_1^2 + v_2^2} \simeq (\sqrt{2}\, G_F)^{-1/2} = 246$ GeV plays the role of the SM VEV when generating the gauge boson masses.

A global SU(2) transformation in the scalar space (ϕ_1, ϕ_2) takes us to the so-called

Higgs basis (Φ_1, Φ_2), where only one doublet acquires a VEV:

$$\begin{pmatrix} \Phi_1 \\ -\Phi_2 \end{pmatrix} \equiv \frac{1}{v} \begin{bmatrix} v_1 & v_2 \\ v_2 & -v_1 \end{bmatrix} \begin{pmatrix} \phi_1 \\ e^{-i\theta}\phi_2 \end{pmatrix} . \tag{2.1}$$

In this basis, the two doublets are parametrized as

$$\Phi_1 = \begin{bmatrix} G^+ \\ \frac{1}{\sqrt{2}}\,(v + S_1 + iG^0) \end{bmatrix} , \qquad \Phi_2 = \begin{bmatrix} H^+ \\ \frac{1}{\sqrt{2}}\,(S_2 + iS_3) \end{bmatrix} , \tag{2.2}$$

where $G^\pm$ and G^0 denote the Goldstone fields and $\langle H^+ \rangle = \langle G^+ \rangle = \langle G^0 \rangle = \langle S_i \rangle = 0$. The five physical scalars are given by two charged fields $H^\pm(x)$ and three neutral ones $\varphi_i^0(x) = \{h(x), H(x), A(x)\}$, which are related to the S_i fields through an orthogonal transformation $\varphi_i^0(x) = \mathcal{R}_{ij} S_j(x)$. The form of $\mathcal{R}_{ij}$ depends on the scalar potential, which could violate CP in its most general version; in that case the resulting mass eigenstates do not have a definite CP parity.

The most general Yukawa Lagrangian of the 2HDM is given by

$$\mathcal{L}_Y \;=\; -\Big\{ \bar{Q}'_L (\Gamma_1 \phi_1 + \Gamma_2 \phi_2)\, d'_R + \bar{Q}'_L (\Delta_1 \widetilde{\phi}_1 + \Delta_2 \widetilde{\phi}_2)\, u'_R + \bar{L}'_L (\Pi_1 \phi_1 + \Pi_2 \phi_2)\, l'_R \Big\} \;+\; \text{h.c.} , \tag{2.3}$$

where $\bar{Q}'_L$ and $\bar{L}'_L$ are the left-handed quark and lepton doublets, respectively, and $\tilde{\phi}_a(x) \equiv i\tau_2 \phi_a^*(x)$ the charge-conjugated scalar doublets with $Y = -\frac{1}{2}$. All fermionic fields are written as N_G-dimensional vectors and the couplings Γ_a, Δ_a and Π_a are $N_G \times N_G$ complex matrices in flavour space, N_G being the number of fermion generations. Moving to the Higgs basis, the Lagrangian reads

$$\begin{aligned} \mathcal{L}_Y \;=\; & -\frac{\sqrt{2}}{v} \Big\{ \bar{Q}'_L (M'_d \Phi_1 + Y'_d \Phi_2)\, d'_R + \bar{Q}'_L (M'_u \tilde{\Phi}_1 + Y'_u \tilde{\Phi}_2)\, u'_R + \bar{L}'_L (M'_l \Phi_1 + Y'_l \Phi_2)\, l'_R \Big\} + \\ & + \text{h.c.} , \end{aligned} \tag{2.4}$$

with

$$M'_d = \frac{1}{\sqrt{2}} \left(v_1 \Gamma_1 + v_2 \Gamma_2 \mathrm{e}^{i\theta} \right) , \qquad Y'_d = \frac{1}{\sqrt{2}} \left(v_1 \Gamma_2 \mathrm{e}^{i\theta} - v_2 \Gamma_1 \right) , \tag{2.5}$$

$$M'_u = \frac{1}{\sqrt{2}} \left(v_1 \Delta_1 + v_2 \Delta_2 \mathrm{e}^{-i\theta} \right) , \qquad Y'_u = \frac{1}{\sqrt{2}} \left(v_1 \Delta_2 \mathrm{e}^{-i\theta} - v_2 \Delta_1 \right) , \tag{2.6}$$

$$M'_l = \frac{1}{\sqrt{2}} \left(v_1 \Pi_1 + v_2 \Pi_2 \mathrm{e}^{i\theta} \right) , \qquad Y'_l = \frac{1}{\sqrt{2}} \left(v_1 \Pi_2 \mathrm{e}^{i\theta} - v_2 \Pi_1 \right) . \tag{2.7}$$

In general, the complex matrices M'_f and Y'_f $(f = d, u, l)$ cannot be simultaneously diagonalized. Thus, in the fermion mass-eigenstate basis, with diagonal mass matrices M_f, the Yukawa-coupling matrices Y_f remain non-diagonal giving rise to FCNC interactions.

The unwanted non-diagonal neutral couplings can be eliminated requiring the alignment in flavour space of the Yukawa matrices [1]. It is convenient to implement this condition in the form:

$$\Gamma_2 = \xi_d \, \mathrm{e}^{-i\theta} \, \Gamma_1 , \qquad \Delta_2 = \xi_u^* \, \mathrm{e}^{i\theta} \Delta_1 , \qquad \Pi_2 = \xi_l \, \mathrm{e}^{-i\theta} \, \Pi_1 , \tag{2.8}$$

Model	(ξ_d, ξ_u, ξ_l)	ς_d	ς_u	ς_l
Type I	(∞, ∞, ∞)	$\cot\beta$	$\cot\beta$	$\cot\beta$
Type II	$(0, \infty, 0)$	$-\tan\beta$	$\cot\beta$	$-\tan\beta$
Type X	$(\infty, \infty, 0)$	$\cot\beta$	$\cot\beta$	$-\tan\beta$
Type Y	$(0, \infty, \infty)$	$-\tan\beta$	$\cot\beta$	$\cot\beta$
Inert	$(\tan\beta, \tan\beta, \tan\beta)$	0	0	0

Table 1: Limits on ξ_f that recover the different $\mathcal{Z}_2$ models and corresponding ς_f values.

where ξ_f are arbitrary complex parameters. The proportionality of the matrices Y'_f and M'_f guarantees that all FCNC couplings vanish at tree level:

$$Y_{d,l} = \varsigma_{d,l} M_{d,l} \,, \qquad Y_u = \varsigma_u^* M_u \,, \qquad \varsigma_f \equiv \frac{\xi_f - \tan\beta}{1 + \xi_f \tan\beta} \,, \qquad \tan\beta \equiv v_2/v_1 \,. \tag{2.9}$$

In the A2HDM the mass-eigenstate Yukawa Lagrangian reads [1]

$$\begin{aligned} \mathcal{L}_Y = & -\frac{\sqrt{2}}{v} H^+(x) \left\{ \bar{u}(x) \left[\varsigma_d \, V M_d \mathcal{P}_R - \varsigma_u \, M_u^\dagger V \mathcal{P}_L \right] d(x) \, + \, \varsigma_l \, \bar{\nu}(x) M_l \mathcal{P}_R l(x) \right\} - \\ & - \frac{1}{v} \sum_{\varphi, f} y_f^{\varphi_i^0} \, \varphi_i^0(x) \, \bar{f}(x) \, M_f \mathcal{P}_R f(x) \, + \, \text{h.c.} \,, \end{aligned} \tag{2.10}$$

where V denotes the CKM matrix, $\mathcal{P}_{R,L} \equiv \frac{1 \pm \gamma_5}{2}$ are the right-handed and left-handed projectors and the couplings of the neutral scalar fields are given by:

$$y_{d,l}^{\varphi_i^0} = \mathcal{R}_{i1} + (\mathcal{R}_{i2} + i \, \mathcal{R}_{i3}) \, \varsigma_{d,l} \,, \qquad\qquad y_u^{\varphi_i^0} = \mathcal{R}_{i1} + (\mathcal{R}_{i2} - i \, \mathcal{R}_{i3}) \, \varsigma_u^* \,. \tag{2.11}$$

Some conclusions can be drawn from (2.10). In the A2HDM all fermionic couplings to scalars are proportional to the corresponding fermion masses and the neutral-current interactions are diagonal in flavour. The only source of flavour-changing interactions is the CKM matrix in the quark charged current, while all leptonic couplings are diagonal in flavour because of the absence of right-handed neutrinos in our framework, which could however easily be included. There are only three new parameters ς_f, which encode all possible freedom allowed by the alignment conditions; these couplings satisfy universality among the different generations, i.e. all fermions with a given electric charge have the same universal coupling ς_f. The three parameters ς_f are also invariant under global SU(2) transformations of the scalar fields $\phi_a \to \phi'_a = U_{ab}\phi_b$ [25], i.e. they are scalar-basis independent. Taking the particular values shown in table 1, the different models based on $\mathcal{Z}_2$ symmetries are recovered, with a single scalar doublet coupling to each type of right-handed fermions [4]. Finally, it should be pointed out again that ς_f are arbitrary complex numbers, opening the possibility of having new sources of CP violation without tree-level FCNCs.

2.1 Quantum corrections

Quantum corrections induce some misalignment of the Yukawa coupling matrices, generating small FCNC effects suppressed by the corresponding loop factors. However, the special

structure of the A2HDM strongly constrains the possible FCNC interactions [1]. Obviously, the alignment condition remains stable under renormalization when it is protected by a $\mathcal{Z}_2$ symmetry [26], i.e. for the particular cases indicated in table 1. In the most general case loop corrections do generate some FCNC effects, but the resulting structures are enforced to satisfy the flavour symmetries of the model. The Lagrangian of the A2HDM is invariant under flavour-dependent phase transformations of the fermion mass eigenstates ($f = d, u, l, \nu$, $X = L, R$, $\alpha_i^{\nu,L} = \alpha_i^{l,L}$):

$$f_X^i(x) \,\to\, \mathrm{e}^{i\alpha_i^{f,X}}\, f_X^i(x)\,, \quad V_{ij} \,\to\, \mathrm{e}^{i\alpha_i^{u,L}} V_{ij}\, \mathrm{e}^{-i\alpha_j^{d,L}}\,, \quad M_{f,ij} \,\to\, \mathrm{e}^{i\alpha_i^{f,L}} M_{f,ij}\, \mathrm{e}^{-i\alpha_j^{f,R}}\,. \quad (2.12)$$

Owing to this symmetry, lepton-flavour-violating neutral couplings are identically zero to all orders in perturbation theory, while in the quark sector the CKM mixing matrix remains the only possible source of flavour-changing transitions. The only allowed local FCNC structures are of the type $\bar{u}_L V (M_d M_d^\dagger)^n V^\dagger (M_u M_u^\dagger)^m M_u u_R$, $\bar{d}_L V^\dagger (M_u M_u^\dagger)^n V (M_d M_d^\dagger)^m M_d d_R$, or similar structures with additional factors of V, $V^\dagger$ and quark mass matrices [1]. Therefore, at the quantum level the A2HDM provides an explicit implementation of the popular Minimal Flavour Violation scenarios [27, 28, 29, 30, 31, 32], but allowing at the same time for new CP-violating phases.[1] Structures of this type have been recently discussed in [33].

Using the renormalization-group equations [26, 34], one can easily check that the one-loop gauge corrections preserve the alignment while the only FCNC structures induced by the scalar contributions take the form [35]:

$$\begin{aligned}\mathcal{L}_{\mathrm{FCNC}} = {} & \frac{C(\mu)}{4\pi^2 v^3}\,(1+\varsigma_u^*\varsigma_d)\;\times \\ & \times \sum_i \varphi_i^0(x)\,\Big\{(\mathcal{R}_{i2}+i\,\mathcal{R}_{i3})\,(\varsigma_d-\varsigma_u)\,\Big[\bar{d}_L\,V^\dagger M_u M_u^\dagger\,V M_d\,d_R\Big] - \\ & \qquad -(\mathcal{R}_{i2}-i\,\mathcal{R}_{i3})\,(\varsigma_d^*-\varsigma_u^*)\,\Big[\bar{u}_L\,V M_d M_d^\dagger\,V^\dagger M_u\,u_R\Big]\Big\}\;+\;\mathrm{h.c.}\end{aligned} \quad (2.13)$$

As they should, these FCNC effects vanish identically when $\varsigma_d = \varsigma_u$ ($\mathcal{Z}_2$ models of type I, X and Inert) or $\varsigma_d = -1/\varsigma_u^*$ (types II and Y). The leptonic coupling ς_l does not induce any FCNC interaction, independently of its value; the usually adopted $\mathcal{Z}_2$ symmetries are unnecessary in the lepton sector. Assuming the alignment to be exact at some scale μ_0, i.e. $C(\mu_0) = 0$, a non-zero value for the FCNC coupling, $C(\mu) = -\log(\mu/\mu_0)$, is generated when running to a different scale.

The numerical effect of these contributions is, in any case, suppressed by $m_q m_{q'}^2/v^3$ and quark-mixing factors. This implies an interesting hierarchy of FCNC effects, avoiding the stringent experimental constraints for light-quark systems, while allowing at the same time for potential interesting signals in heavy-quark transitions. Obviously, the most relevant terms in (2.13) are the $\bar{s}_L b_R$ and $\bar{c}_L t_R$ operators. The $\bar{s}_L b_R$ term induces a calculable contribution to B_s^0–$\bar{B}_s^0$ mixing through φ_i^0 exchanges, which modifies the mixing phase and could explain the like-sign dimuon charge asymmetry recently observed by D0 [36]. Tree-level scalar exchanges from FCNC vertices have been already suggested as a possible

[1] Minimal flavour violation within the context of the Type II 2HDM has been discussed in [27]. This reference didn't consider the possibility of incorporating new CP-violating phases.

explanation of the D0 measurement [37]. We defer the phenomenological analysis of the FCNC operator (2.13) to a future publication [35], where the neutral sector of the A2HDM will be studied in detail. In the present paper we will concentrate in the phenomenology of the charged-scalar Yukawa Lagrangian (2.10).

3. Inputs and statistical treatment

In the following sections we will analyze the most important flavour-changing processes that are sensitive to charged-scalar exchange and will try to constrain from them the new-physics parameters ς_f. Most of these observables have been discussed in recent phenomenological analyses, usually in the framework of the type II 2HDM [38, 39, 40, 41], but also in the type III 2HDM [42].

For that purpose, a good control of the hadronic decay parameters is necessary. These usually involve large theoretical uncertainties whose treatment is not well defined. In our work we use the statistical approach RFit [43], which has been implemented in the CKMfitter package [44]. The new-physics parameter space is explored, assigning to each point the maximal relative likelihood under variation of the theoretical parameters which are not shown. Theoretical uncertainties are treated by defining allowed ranges within which the contribution of the corresponding theoretical quantity to the $\Delta\chi^2$ is set to zero, while it is set to infinity outside. This treatment implies that uncertainties of this kind should be chosen conservatively and added linearly.

Another related problem is the combination of different theoretical determinations of a hadronic quantity, which is even less well defined. We follow the prescription given in [44]. However, unless commented explicitly, we only take lattice results coming from numerical simulations with 2+1 flavours. For quantities concerning the light hadrons, we consider the determinations recommended by the Flavour Lattice Averaging Group (FLAG) [45, 46]. The obtained values are collected in table 2.

For $f_+^{K\pi}(0)$ the only published value with 2+1 dynamical quarks is the one from RBC/UKQCD [47, 48], which however fails to fulfill the FLAG standards. On the other hand, there is one 2-flavour result, which fulfills the FLAG criteria [49]. Although consistent with the old Leutwyler-Roos estimate [50], based on $O(p^4)$ Chiral Perturbation Theory (χPT), these lattice determinations are somewhat smaller than the $O(p^6)$ analytical calculations [51, 52, 53, 54]. We take this into account and adopt the conservative range $f_+^{K\pi}(0) = 0.965 \pm 0.010$.

To fix the values of the relevant CKM entries we only use determinations [64, 79, 80] which are not sensitive to the new-physics contributions. Thus, we use the V_{ud} value extracted from superallowed ($0^+ \to 0^+$) nuclear β decays and CKM unitarity to determine $V_{us} \equiv \lambda$. The values of V_{ub} and $V_{cb} = A\lambda^2$ are determined from exclusive and inclusive $b \to u l \bar{\nu}_l$ and $b \to c l \bar{\nu}_l$ transitions, respectively, with $l = e, \mu$. The apex $(\bar{\rho}, \bar{\eta})$ of the unitarity triangle has been determined from $|V_{ub}/V_{cb}|$, λ and the ratio $\Delta m_{B_s^0}/\Delta m_{B_d^0}$ (see section 5.2). For the top quark mass we have adopted the usual assumption that the Tevatron value [67] corresponds to the pole mass, but increasing its systematic error by 1 GeV to account for the intrinsic ambiguity in the m_t definition; i.e. we have taken

Parameter	Value	Comment
f_{B_s}	$(0.242 \pm 0.003 \pm 0.022)$ GeV	Our average [55, 56, 57]
f_{B_s}/f_{B_d}	$1.232 \pm 0.016 \pm 0.033$	Our average [56, 57]
f_{D_s}	$(0.2417 \pm 0.0012 \pm 0.0053)$ GeV	Our average [55, 58, 57]
f_{D_s}/f_{D_d}	$1.171 \pm 0.005 \pm 0.02$	Our average [58, 57]
f_K/f_π	$1.192 \pm 0.002 \pm 0.013$	Our average [58, 59, 60]
$f_{B_s}\sqrt{\hat{B}_{B_s^0}}$	$(0.266 \pm 0.007 \pm 0.032)$ GeV	[56]
$f_{B_d}\sqrt{\hat{B}_{B_s^0}}/(f_{B_s}\sqrt{\hat{B}_{B_s^0}})$	$1.258 \pm 0.025 \pm 0.043$	[56]
$\hat{B}_K$	$0.732 \pm 0.006 \pm 0.043$	[61, 62]
$\lvert V_{ud}\rvert$	0.97425 ± 0.00022	[63]
λ	0.2255 ± 0.0010	$\left(1 - \lvert V_{ud}\rvert^2\right)^{1/2}$
$\lvert V_{ub}\rvert$	$(3.8 \pm 0.1 \pm 0.4) \cdot 10^{-3}$	$b \to ul\nu$ (excl. + incl.) [64, 65]
A	$0.80 \pm 0.01 \pm 0.01$	$b \to cl\nu$ (excl. + incl.) [64, 65]
$\bar{\rho}$	$0.15 \pm 0.02 \pm 0.05$	Our fit
$\bar{\eta}$	$0.38 \pm 0.01 \pm 0.06$	Our fit
$\bar{m}_u(2\text{ GeV})$	$(0.00255\,^{+\,0.00075}_{-\,0.00105})$ GeV	[66]
$\bar{m}_d(2\text{ GeV})$	$(0.00504\,^{+\,0.00096}_{-\,0.00154})$ GeV	[66]
$\bar{m}_s(2\text{ GeV})$	$(0.105\,^{+\,0.025}_{-\,0.035})$ GeV	[66]
$\bar{m}_c(2\text{ GeV})$	$(1.27\,^{+\,0.07}_{-\,0.11})$ GeV	[66]
$\bar{m}_b(m_b)$	$(4.20\,^{+\,0.17}_{-\,0.07})$ GeV	[66]
$\bar{m}_t(m_t)$	$(165.1 \pm 0.6 \pm 2.1)$ GeV	[67]
$\delta_{\rm em}^{K\ell 2/\pi\ell 2}$	-0.0070 ± 0.0018	[68, 69, 70, 71]
$\delta_{\rm em}^{\tau K2/K\ell 2}$	0.0090 ± 0.0022	[72, 73, 74]
$\delta_{\rm em}^{\tau\pi 2/\pi\ell 2}$	0.0016 ± 0.0014	[72, 73, 74]
$\rho^2\vert_{B\to Dl\nu}$	$1.18 \pm 0.04 \pm 0.04$	[65]
$\Delta\vert_{B\to Dl\nu}$	0.46 ± 0.02	[75]
$f_+^{K\pi}(0)$	0.965 ± 0.010	[47, 48, 49, 51, 52, 53, 54]
$\bar{g}^L_{b,SM}$	$-0.42112\,^{+\,0.00035}_{-\,0.00018}$	[76, 77]
κ_ϵ	0.94 ± 0.02	[78]
$\bar{g}^R_{b,SM}$	$0.07744\,^{+\,0.00006}_{-\,0.00008}$	[76, 77]

Table 2: *Input values for the hadronic parameters, obtained as described in the text. The first error denotes statistical uncertainty, the second systematic/theoretical.*

$m_t^{\rm pole} = (173.1 \pm 0.6 \pm 2.1)$ GeV and have converted this value into the running $\overline{\rm MS}$ mass. The measurements used in our analysis are listed in table 3.

Concerning the charged-scalar mass, we will use the LEP lower bound $M_{H^\pm} > 78.6$ GeV (95% CL), which does not refer to any specific Yukawa structure [1, 81]. This limit assumes only that H^+ decays dominantly into $u_i\bar{d}_j$ and $l^+\nu_l$. Obviously, the bound is avoided by a fermiophobic (inert) A2HDM with $\varsigma_f \ll 1$, but all our constraints would also disappear in this case. The charged scalar could still be detected through the decay mode $H^\pm \to W^\pm A$, provided it is kinematically allowed. Assuming a CP-conserving scalar po-

Observable	Value	Comment
$\lvert g^S_{RR}\rvert_{\tau\to\mu}$	< 0.72 (95% CL)	[66]
$\mathrm{Br}(\tau \to \mu\nu_\tau\bar{\nu}_\mu)$	$(17.36 \pm 0.05) \times 10^{-2}$	[66]
$\mathrm{Br}(\tau \to e\nu_\tau\bar{\nu}_e)$	$(17.85 \pm 0.05) \times 10^{-2}$	[66]
$\mathrm{Br}(\tau \to \mu\nu_\tau\bar{\nu}_\mu)/\mathrm{Br}(\tau \to e\nu_\tau\bar{\nu}_e)$	0.9796 ± 0.0039	[83]
$\mathrm{Br}(B \to \tau\nu)$	$(1.73 \pm 0.35) \times 10^{-4}$	[80]
$\mathrm{Br}(D \to \mu\nu)$	$(3.82 \pm 0.33) \times 10^{-4}$	[84]
$\mathrm{Br}(D \to \tau\nu)$	$\leq 1.3 \times 10^{-3}$ (95% CL)	[84]
$\mathrm{Br}(D_s \to \tau\nu)$	$(5.58 \pm 0.35) \times 10^{-2}$	[85, 86, 87, 88, 89]
$\mathrm{Br}(D_s \to \mu\nu)$	$(5.80 \pm 0.43) \times 10^{-3}$	[85, 89, 90]
$\Gamma(K \to \mu\nu)/\Gamma(\pi \to \mu\nu)$	1.334 ± 0.004	[71]
$\Gamma(\tau \to K\nu)/\Gamma(\tau \to \pi\nu)$	$(6.50 \pm 0.10) \times 10^{-2}$	[66, 83]
$\log C$	0.194 ± 0.011	[91, 92]
$\mathrm{Br}(B \to D\tau\nu)/BR(B \to D\ell\nu)$	0.392 ± 0.079	[93, 94, 95]
$\Gamma(Z \to b\bar{b})/\Gamma(Z \to \mathrm{hadrons})$	0.21629 ± 0.00066	[96]
$\mathrm{Br}(\bar{B} \to X_s\gamma)_{E_\gamma > 1.6\mathrm{GeV}}$	$(3.55 \pm 0.26) \times 10^{-4}$	[65]
$\mathrm{Br}(\bar{B} \to X_c e\bar{\nu}_e)$	$(10.74 \pm 0.16) \times 10^{-2}$	[65]
$\Delta m_{B^0_d}$	$(0.507 \pm 0.005)\ \mathrm{ps}^{-1}$	[65]
$\Delta m_{B^0_s}$	$(17.77 \pm 0.12)\ \mathrm{ps}^{-1}$	[65]
$\lvert\epsilon_K\rvert$	$(2.228 \pm 0.011) \times 10^{-3}$	[66]

Table 3: *Measurements used in the analysis. Masses and lifetimes are taken from the PDG [66].*

tential, OPAL finds the 95% CL constraints $M_{H^\pm} > 56.5$ (64.8) GeV, for 12 (15) GeV $< M_A < M_{H^\pm} - M_{W^\pm}$ [82].

4. Tree-level decays

4.1 Lepton decays

The pure leptonic decays $l \to l'\bar{\nu}_{l'}\nu_l$ provide accurate tests of the universality of the leptonic W couplings and of their left-handed current structure [66, 97, 98]. The exchange of a charged scalar induces an additional amplitude mediating the decay of a right-handed initial lepton into a right-handed final charged lepton; in standard notation [98, 99], this scalar contribution gets parametrized through the effective low-energy coupling $g^S_{RR} = -\frac{m_l m_{l'}}{M^2_{H^\pm}} |\varsigma_l|^2$. Its phenomenological effects can be isolated through the Michel parameters governing the decay distribution,

$$\rho - \frac{3}{4} = 0\,, \quad \eta = \frac{1}{2N}\,\mathrm{Re}(g^S_{RR})\,, \quad \xi - 1 = -\frac{1}{2N}\,|g^S_{RR}|^2\,, \quad \xi\delta - \frac{3}{4} = -\frac{3}{8N}\,|g^S_{RR}|^2\,, \quad (4.1)$$

and in the total decay width

$$\Gamma(l \to l'\ \bar{\nu}_{l'}\ \nu_l) = \frac{G_F^2}{192\pi^3}\ m_l^5\ N\ \ \left[f\left(\frac{m^2_{l'}}{m^2_l}\right) + 4\ \eta\ \frac{m_{l'}}{m_l}\ g\left(\frac{m^2_{l'}}{m^2_l}\right)\right]\ r_{\mathrm{RC}}\,, \qquad (4.2)$$

where $f(x) = 1 - 8x + 8x^3 - x^4 - 12x^2 \log x$, $g(x) = 1 + 9x - 9x^2 - x^3 + 6x(1+x)\log x$, $N = 1 + \frac{1}{4}|g^S_{RR}|^2$ and [100]

$$r_{\rm RC} = \left[1 + \frac{\alpha(m_l)}{2\pi}\left(\frac{25}{4} - \pi^2\right)\right]\left[1 + \frac{3}{5}\frac{m_l^2}{M_W^2} - 2\frac{m_{l'}^2}{M_W^2}\right]. \tag{4.3}$$

Since the scalar couplings are proportional to lepton masses, the decay $\tau \to \mu\bar{\nu}_\mu\nu_\tau$ is the most sensitive one to the scalar-exchange contribution. The present bound $|g^S_{RR}|_{\tau\to\mu} < 0.72$ (95% CL) [66] translates into $|\varsigma_l|/M_{H^\pm} \leq 1.96$ GeV^{-1} (95% CL). A better limit can be obtained from the ratio of the total τ decay widths into the muon and electron modes. The universality test $|g_\mu/g_e|^2 \equiv |{\rm Br}(\tau\to\mu)/{\rm Br}(\tau\to e)||f(m_e^2/m_\tau^2)/f(m_\mu^2/m_\tau^2)| = 1.0036 \pm 0.0029$ [66, 83] implies:

$$\frac{|\varsigma_l|}{M_{H^\pm}} \;\leq\; 0.40 \text{ GeV}^{-1} \qquad (95\%\,\text{CL}). \tag{4.4}$$

4.2 Leptonic decays of pseudoscalar mesons

Information about new-physics parameters can be also extracted from leptonic decays of pseudoscalar mesons, $P^+ \to l^+\nu_l$, which are very sensitive to H^+ exchange due to the helicity suppression of the SM amplitude. The total decay width is given by[2]

$$\Gamma(P^+_{ij} \to l^+\nu_l) \;=\; G_F^2 m_l^2 f_P^2 |V_{ij}|^2 \frac{m_{P^+_{ij}}}{8\pi}\left(1 - \frac{m_l^2}{m^2_{P^+_{ij}}}\right)^2 (1 + \delta^{M\ell 2}_{\rm em})\,|1 - \Delta_{ij}|^2\,, \tag{4.5}$$

where i, j represent the valence quarks of the meson under consideration. The correction

$$\Delta_{ij} \;=\; \left(\frac{m_{P^\pm_{ij}}}{M_{H^\pm}}\right)^2 \varsigma_l^* \,\frac{\varsigma_u m_{u_i} + \varsigma_d m_{d_j}}{m_{u_i} + m_{d_j}} \tag{4.6}$$

encodes the new-physics information and $\delta^{M\ell 2}_{\rm em}$ denotes the electromagnetic radiative contributions. These corrections are relevant because the additional photon lifts the helicity suppression of the two-body decay, thereby compensating in part for the additional electromagnetic coupling, and the two processes are not distinguishable experimentally for low photon energies. Their relative importance therefore increases for decreasing lepton masses.

The correction Δ_{ij} is predicted to be positive in model I, negative in model X and can have either sign in the models II and Y, depending on the decaying meson, while it is of course absent in the *inert* scenario. In the more general A2HDM it is a complex number with a real part of either sign. To determine its size one needs to know $|V_{ij}|$ and a theoretical determination of the meson decay constant.

The SM as well as the 2HDM contribution to this class of decays start at tree level. Therefore they can be assumed to remain the dominant contributions, relatively independent of a possible high-energy completion of the theory. Electroweak loop corrections are of course expected and they could be sizeable in some cases, for example in supersymmetry at large values of $\tan\beta$ [101, 102].

[2]The normalization of the meson decay constant corresponds to $f_\pi = \sqrt{2}F_\pi = 131$ MeV.

4.2.1 Heavy pseudoscalar mesons

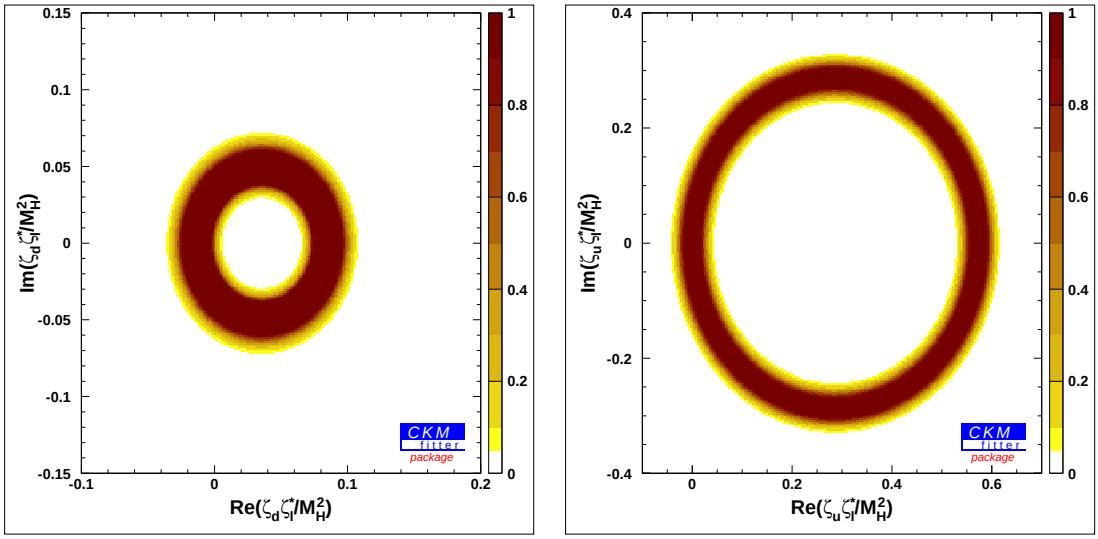

Figure 1: *Constraints in the complex $\varsigma_l^* \varsigma_{u,d}/M_{H^\pm}^2$ planes from $B \to \tau\nu$ (left) and $D \to \mu\nu$ (right), in units of GeV^{-2}. The colour code indicates confidence levels $(1 - CL)$.*

The leptonic decays of heavy pseudoscalar mesons that have been measured up to now are $B \to \tau\nu$, $D_s \to \mu\nu$, $D_s \to \tau\nu$ and $D \to \mu\nu$. The radiative corrections for the leptonic decays of heavy mesons have been estimated in [103], and are already taken into account in the experimental values given in table 3; therefore the electromagnetic correction is set to zero in Eq. (4.5).

In B and D decays the function Δ_{ij} can be approximated by neglecting the contribution proportional to the light quark mass, because $m_u/m_b \lesssim m_d/m_c \sim \mathcal{O}(10^{-3})$. Therefore the relations

$$\Delta_{ub} \approx \frac{m_B^2}{M_{H^\pm}^2} \varsigma_l^* \varsigma_d \,, \qquad \Delta_{cd} \approx \frac{m_D^2}{M_{H^\pm}^2} \varsigma_l^* \varsigma_u \tag{4.7}$$

hold, leading to a direct constraint on these combinations. While for $D_{(s)} \to \tau\nu$ the helicity suppression is absent, the corresponding phase space is small and there are two neutrinos in the final state, which is why $D \to \tau\nu$ has not been measured up to now. Nevertheless, the upper limit set by CLEO [84] starts to become relevant in constraining our parameters: $|1-\Delta_{cd}| < 1.19$ (95% CL). The present experimental limit on $B \to \mu\nu$ gives $|1-\Delta_{ub}| < 2.04$ (95% CL). The information obtained from the decays $B \to \tau\nu$ and $D \to \mu\nu$ is shown in figure 1. The broad dark red (black) ring in the middle reflects the fact, that the systematic error is dominant in these constraints, leading to a large amount of degeneracy for the 'best fit value'. To infer a limit at a certain confidence level, the corresponding number of rings has to be included, for example for 95% up to the yellow (light grey) corresponding to $1 - CL = 0.05$. The resulting 95% CL constraints, $|1 - \Delta_{ub}| \in [0.8, 2.0]$ and $|1-\Delta_{cd}| \in [0.87, 1.12]$, translate into allowed circular bands in the $\varsigma_l^* \varsigma_{u,d}/M_{H^\pm}^2$ complex planes. For real Yukawa couplings there is a two-fold sign ambiguity generating two possible

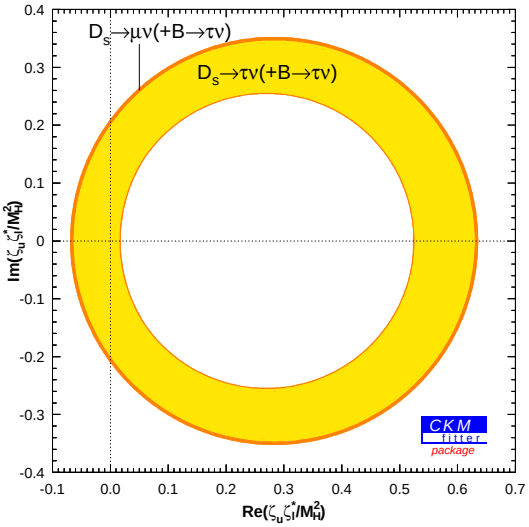

Figure 2: *95% CL constraints in the complex $\varsigma_l^*\varsigma_u/M^2_{H^\pm}$ plane from $D_s \to (\tau,\mu)\nu$, in units of GeV^{-2}, using $B \to \tau\nu$ to constrain $\varsigma_l^*\varsigma_d/M^2_{H^\pm}$.*

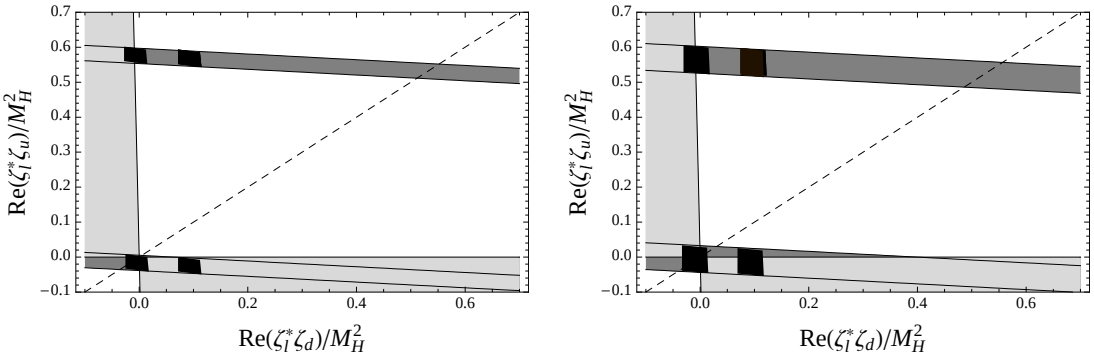

Figure 3: *Constraints from $D_s \to \tau\nu_\tau$ (left) and $D_s \to \mu\nu_\mu$ (right), in units of GeV^{-2}, under the assumption of real parameters ς_f. The grey bands correspond to 95% CL. Also shown are the cuts for the 2HDM of type I/X (dashed line) and II (lighter grey area, $\tan\beta \in [0.1, 60]$). Finally, the four black regions are the possible allowed areas considering the information coming from $B \to \tau\nu_\tau$.*

solutions, the expected one around $\Delta_{ij} = 0$ (the SM amplitude dominates) and its mirror around $\Delta_{ij} = 2$, corresponding to a new-physics contribution twice as large as the SM one and of opposite sign. The real solutions are $\varsigma_l^*\varsigma_d/M^2_{H^\pm} \in [-0.036, 0.008]$ GeV^{-2} and $[0.064, 0.108]$ GeV^{-2}, and $\varsigma_l^*\varsigma_u/M^2_{H^\pm} \in [-0.037, 0.037]$ GeV^{-2} and $[0.535, 0.609]$ GeV^{-2}.

In D_s decays we get $|1 - \Delta_{cs}| \in [0.97, 1.18]$ from $D_s \to \mu\nu$ and $|1 - \Delta_{cs}| \in [0.98, 1.16]$ from $D_s \to \tau\nu$. Here the situation is a bit more complex, because $m_s/m_c \approx 10\%$ and the light-quark term in the Δ_{cs} function cannot be neglected since this suppression could be compensated by the different ς_f. Therefore there is no direct constraint, neither on $\varsigma_l^*\varsigma_u/M^2_{H^\pm}$ nor on $\varsigma_l^*\varsigma_d/M^2_{H^\pm}$, only a correlation among them. For that reason, we use the additional information from $B \to \tau\nu$ to constrain the parameters which are not shown.

This suffices to render the influence of the mass-suppressed term subdominant.

If CP symmetry were only broken by the CKM phase, the parameters ς_f would be real. In this case, the constraints from $D_s \to \tau\nu_\tau$ and $D_s \to \mu\nu_\mu$ can be visualized as shown in figure 3, plotting the correlation between the two real parameters. The two grey bands are associated with the two possible solutions around $\Delta_{cs} = 0$ and $\Delta_{cs} = 2$. The different models with $\mathcal{Z}_2$-symmetry correspond to cuts in these plots. The plots show the small influence of the term proportional to the strange quark mass, as long as the couplings are of the same order. Using the constraints on $\varsigma_l^* \varsigma_d / M_{H^\pm}^2$ from $B \to \tau\nu$, one finds for the other coupling combination the two real solutions $\varsigma_l^* \varsigma_u / M_{H^\pm}^2 \in [-0.005, 0.041]$ GeV^{-2} and $[0.511, 0.557]$ GeV^{-2}, at 95% CL, which agree with the corresponding constraints from $D \to \mu\nu$. Putting together all the information from leptonic B, D and D$_s$ decays, the real solutions are:

$$\frac{\varsigma_l^* \varsigma_d}{M_{H^\pm}^2} \in \begin{cases} [-0.036, 0.008] \text{ GeV}^{-2}, \\ [0.064, 0.108] \text{ GeV}^{-2}, \end{cases} \qquad \frac{\varsigma_l^* \varsigma_u}{M_{H^\pm}^2} \in \begin{cases} [-0.006, 0.037] \text{ GeV}^{-2}, \\ [0.511, 0.535] \text{ GeV}^{-2}. \end{cases} \tag{4.8}$$

4.2.2 Light pseudoscalar mesons

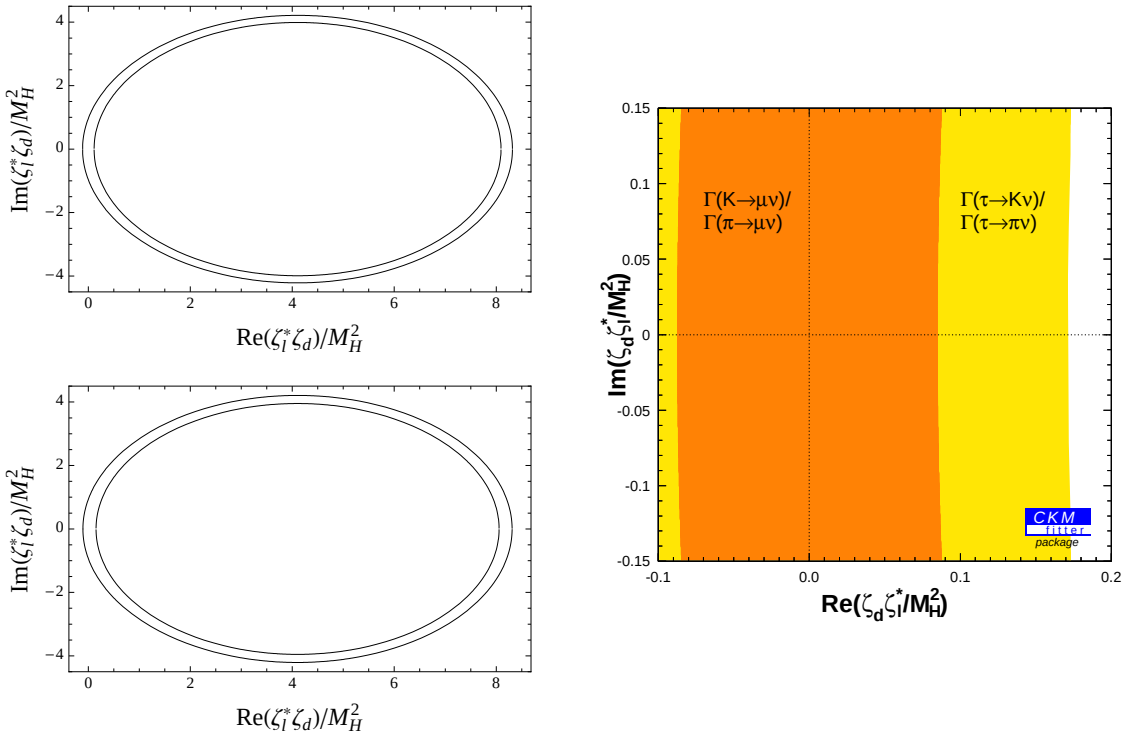

Figure 4: *Constraints in the complex plane $(\varsigma_l^* \varsigma_d)/M_{H^\pm}^2$, in units of GeV^{-2}. Left: Full regions allowed at 95% CL for $K/\pi \to \mu\nu$ (upper plot) and $\tau \to K/\pi\nu$ (lower plot). Right: 95% CL constraints in the interesting region (from the global fit) for both constraints, using $D \to \mu\nu$ to constrain $\varsigma_l^* \varsigma_u / M_{H^\pm}^2$.*

Due to the cancellation of common uncertainties, lattice calculations of the ratio f_K/f_π are more precise than the determinations of the individual decay constants. This ratio can

be extracted experimentally from two different ratios of decay widths:

$$\frac{\Gamma(K\to\mu\nu)}{\Gamma(\pi\to\mu\nu)} = \frac{m_K}{m_\pi}\left(\frac{1-m_\mu^2/m_K^2}{1-m_\mu^2/m_\pi^2}\right)^2 \left|\frac{V_{us}}{V_{ud}}\right|^2 \left(\frac{f_K}{f_\pi}\right)^2 (1+\delta_{\rm em}^{Kl2/\pi l2}) \left|\frac{1-\Delta_{us}}{1-\Delta_{ud}}\right|^2 , \quad (4.9)$$

$$\frac{\Gamma(\tau\to K\nu)}{\Gamma(\tau\to\pi\nu)} = \left(\frac{1-m_K^2/m_\tau^2}{1-m_\pi^2/m_\tau^2}\right)^2 \left|\frac{V_{us}}{V_{ud}}\right|^2 \left(\frac{f_K}{f_\pi}\right)^2 (1+\delta_{\rm em}^{\tau K2/\tau\pi 2}) \left|\frac{1-\Delta_{us}}{1-\Delta_{ud}}\right|^2 , \quad (4.10)$$

where $\delta_{\rm em}^{Kl2/\pi l2}$ is given in table 2 and $\delta_{\rm em}^{\tau K2/\tau\pi 2} = \delta_{\rm em}^{(\tau K2/K\ell 2)} + \delta_{\rm em}^{K\ell 2/\pi\ell 2} - \delta_{\rm em}^{\tau\pi 2/\pi\ell 2} = 0.0004 \pm 0.0054$.

The new-physics corrections are dominated by $\Delta_{us} \simeq \varsigma_l^* \varsigma_d m_K^2/M_{H^\pm}^2$. As $m_K^2/m_B^2 \sim 1\%$, the scalar contributions to these decays are much smaller than for the heavy mesons. However, the good experimental precision achieved provides interesting constraints, as shown in figure 4, which are dominated by the $K_{\mu 2}/\pi_{\mu 2}$ ratio. At 95% CL, one finds $|1-\Delta_{us}| \in [0.984, 1.017]$ from $K_{\mu 2}/\pi_{\mu 2}$ and $|1-\Delta_{us}| \in [0.965, 1.025]$ from the ratio $\tau \to \nu K/\pi$. The real solutions are then, $\varsigma_l^* \varsigma_d / M_{H^\pm}^2 \in [-0.07, 0.07]$ GeV^{-2} or $[8.14, 8.28]$ GeV^{-2}. The larger real solution is already excluded by the $B \to \tau\nu$ data.

4.3 Semileptonic decays of pseudoscalar mesons

Semileptonic decays receive contributions from a charged scalar as well, but in this case the leading SM amplitude is not helicity suppressed, therefore the relative influence is smaller. In addition, there are momentum-dependent form factors involved. The decay amplitude $M \to M' l \bar{\nu}_l$ is characterized by two form factors, $f_+(t)$ and $f_0(t)$ associated with the P-wave and S-wave projections of the crossed-channel matrix element $\langle 0|\bar{u}_i \gamma^\mu d_j|M\bar{M}'\rangle$. The scalar-exchange amplitude only contributes to the scalar form factor; it amounts to a multiplicative correction

$$\tilde{f}_0(t) \;=\; f_0(t)\;(1+\delta_{ij}\,t)\;, \quad (4.11)$$

where

$$\delta_{ij} \;\equiv\; -\frac{\varsigma_l^*}{M_{H^\pm}^2}\,\frac{\varsigma_u m_{u_i} - \varsigma_d m_{d_j}}{m_{u_i} - m_{d_j}}\,. \quad (4.12)$$

The determination of the CKM matrix element $|V_{ij}|$ is not contaminated by the new-physics contribution, because it is governed by the vector form factor. One measures the electron mode $M \to M' e \bar{\nu}_e$, where the scalar contribution is heavily suppressed by the electron mass, determining the product $|V_{ij}|\,|f_+(t_0)|$, with $t_0 = 0$ for light-quark transitions and $t_0 = (m_M - m_{M'})^2$ for heavy quarks. A theoretical calculation of $|f_+(t_0)|$ is then needed to extract $|V_{ij}|$. The sensitivity to the scalar contribution can only be achieved in semileptonic decays into heavier leptons. Whenever available, one can make use of the differential decay distribution to separate the scalar and vector amplitudes. In any case, theoretical determinations of the scalar and vector form factors are needed to extract information on δ_{ij}.

4.3.1 $B \to D\tau\nu_\tau$

To reduce the uncertainty from the vector form factor, let us consider the ratio

$$\frac{\mathrm{Br}(B\to D\tau\nu_\tau)}{\mathrm{Br}(B\to De\nu_e)} \;=\; a_0 + a_1\left(m_B^2 - m_D^2\right)\mathrm{Re}(\delta_{cb}) + a_2\left(m_B^2 - m_D^2\right)^2 |\delta_{cb}|^2\,. \quad (4.13)$$

The coefficients a_i, which contain the dependence on the strong-interaction dynamics, have been studied recently and parametrized in terms of the vector form-factor slope ρ^2 and the scalar density $\Delta(v_B \cdot v_D) \equiv \Delta$, assumed to be constant [39, 104]. We make use of these parametrizations, taking for the two parameters the values indicated in table 2. The function $\Delta(v_B \cdot v_D) \propto f_0(t)/f_+(t)$ has been studied in the lattice, in the range $v_B \cdot v_D = 1$–1.2, and found to be consistent with a constant value $\Delta = 0.46 \pm 0.02$, very close to its static-limit approximation $(m_B - m_D)/(m_B + m_D)$ [75].

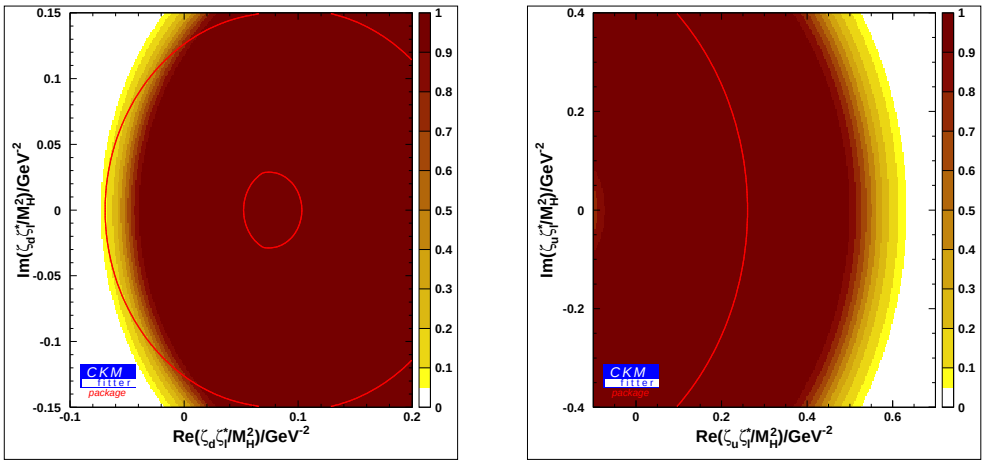

Figure 5: *Constraints from $B \to D\tau\nu_\tau$, in units of GeV^{-2}, plotted in the complex plane for $\varsigma_l^*\varsigma_d/M_{H^\pm}^2$ (left) and $\varsigma_l^*\varsigma_u/M_{H^\pm}^2$ (right), using $D \to \mu\nu$ and $B \to \tau\nu$ to constrain the combination not shown, respectively. The colours indicate $1 - CL$, the red lines the constraint (95% CL) for $\varsigma_l^*\varsigma_{u,d}/M_{H^\pm}^2 \to 0$.*

We obtain once more a correlation between $\varsigma_l^*\varsigma_u/M_{H^\pm}^2$ and $\varsigma_l^*\varsigma_d/M_{H^\pm}^2$, where the term proportional to the charm quark mass is in general potentially more important than in the type II model. The results are shown in figure 5 for both parameter combinations. As can be seen there, the constraint on $\varsigma_d\varsigma_l^*/M_{H^\pm}^2$ is consistent with the information coming from $B \to \tau\nu$ and the leptonic decays of light mesons, but does not constrain this combination further as long as only the information of $B \to D\tau\nu_\tau$ is used. The red lines indicating the constraint for $\varsigma_l^*\varsigma_u \to 0$, however, show that the semileptonic decay can exclude a small region around $(0.08, 0)$, once that combination is bound to be small. We will use this to exclude the second real solution for $\varsigma_l^*\varsigma_d/M_{H^\pm}^2$ with aid of the processes $\epsilon_K, Z \to b\bar{b}$ and $\tau \to \mu\nu\nu$ (see figure 8). Also, when plotted in the complex $\varsigma_l^*\varsigma_u/M_{H^\pm}^2$ plane, it becomes apparent that this constraint is important to exclude the second real solution allowed by $D_{(s)} \to \ell\nu$ decays, already using only the information from leptonic decays in addition (see again figure 8).

Considering the limit of real ς_f's, the correlation between the real parts is visualized in figure 6, together with the cuts corresponding to the different models with $\mathcal{Z}_2$ symmetries. The plot shows that the m_b and m_c terms have potentially similar influence in this case.

It has been pointed out in [105] that measuring the spectrum instead of just the branching ratio will increase the sensitivity of this channel. This, however, has not been

done up to now, due to lack of statistics.

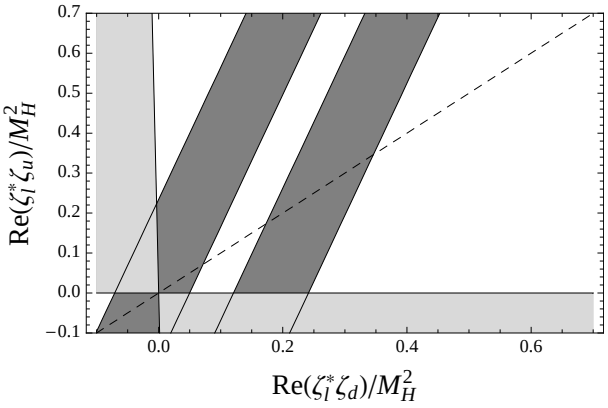

Figure 6: *Allowed regions for $Re(\varsigma_l^*\varsigma_d)/M_{H^\pm}^2$ and $Re(\varsigma_l^*\varsigma_u)/M_{H^\pm}^2$ from the process $B \to D\tau\nu$ at 95% CL (grey), in units of GeV^{-2}, assuming that their imaginary parts are zero. The projections for the 2HDMs of types I/X (dashed line) and II (lighter grey area, $\tan\beta \in [0.1, 60]$) are also shown.*

4.3.2 $K \to \pi\ell\nu$

In semileptonic kaon decays the Callan-Treiman theorem [106, 107] allows to relate the scalar form factor at the kinematic point $t_{\rm CT} = m_K^2 - m_\pi^2$ to the ratio of kaon and pion decay constants: $C \equiv f_0(t_{\rm CT})/f_+(0) = \frac{f_K}{f_\pi}\frac{1}{f_+(0)} + \Delta_{\rm CT}$, where $\Delta_{\rm CT} = (-3.5 \pm 8)\cdot 10^{-3}$ is a small χPT correction of $O[m_\pi^2/(4\pi f_\pi)^2]$ [108, 54, 109]. Using a twice-subtracted dispersion relation for $f_0(t)$ [110], the constant C has been determined from the $K_{\mu 3}$ data by KLOE [91], KTeV [92] and NA48 [111]. In the average quoted in table 3 the NA48 result has been excluded because it disagrees with the other two measurements by more than 2σ.

In the presence of charged-scalar contributions, the scalar form factor gets modified as indicated in Eq. (4.11), inducing a corresponding change in C. Taking into account that the analyzed experimental distribution is only sensitive to $|\tilde{f}_0(t)|^2$, to first order in the new-physics correction δ_{us}, the measured value of C corresponds to

$$\log C = \log\left(\frac{f_K}{f_\pi}\frac{1}{f_+(0)} + \Delta_{CT}\right) + \mathrm{Re}\left[\delta_{us}(m_K^2 - m_\pi^2)\right] . \tag{4.14}$$

The resulting constraint on the real part of $\varsigma_d\varsigma_l^*/M_{H^\pm}^2$ is shown in figure 7, leading to

$$\mathrm{Re}\left(\frac{\varsigma_l^*\varsigma_d}{M_{H^\pm}^2}\right) \in [-0.16, 0.30]\ \mathrm{GeV}^{-2} \quad (95\%\ \mathrm{CL}) , \tag{4.15}$$

which is in agreement with the previous constraints, but with larger uncertainties. This might change in the near future, due to improved lattice determinations of $f_+(0)$ and f_K/f_π, as well as improved experimental precision, e.g. from NA62 or KLOE-2.

4.4 Global fit to leptonic and semileptonic decays

Combining the information from all leptonic and semileptonic decays discussed before, one gets the constraints shown in figure 8. $|\varsigma_d\varsigma_l^*/M_{H^\pm}^2|$ is bounded to be smaller than

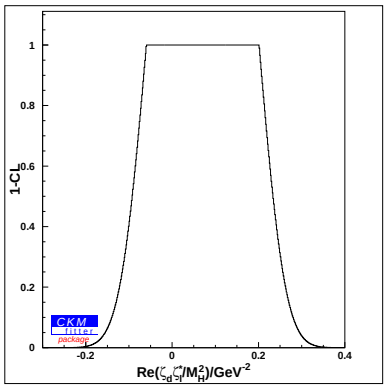

Figure 7: *Constraint from the direct measurement of* $\log C$*, in units of* GeV^{-2}*.*

~ 0.1 GeV^{-2} (95% CL) from these decays alone, while for $\varsigma_u\varsigma_l^*/M_{H^\pm}^2$ the constraints are relatively weak, due to the similar masses of the mesons in the leptonic decays. Note that in both cases there are two real solutions. For the combination $\varsigma_u\varsigma_l^*/M_{H^\pm}^2$, one real solution is excluded in the global fit at 95% CL, while the other, including the SM point of vanishing couplings remains allowed. As mentioned before, this exclusion is due to $B \to D\tau\nu$ in combination with the constraint on $\varsigma_d\varsigma_l^*/M_{H^\pm}^2$. For the latter, the situation is more complicated. The second solution remains allowed, due to the overlapping of the two main constraints in both regions and the weak constraint on $\varsigma_u\varsigma_l^*/M_{H^\pm}^2$ derived from semileptonic decays. However, using in addition the information coming from leptonic τ decays in (4.4), the lower Higgs mass bound from LEP and the constraint from $\epsilon_K, Z \to \bar{b}b$ (see section 5.1) in a conservative way, $|\varsigma_u\varsigma_l^*|/M_{H^\pm}^2 \lesssim 0.01$ GeV^{-2}, the second real solution for $\varsigma_d\varsigma_l^*/M_{H^\pm}^2$ is excluded as well by $B \to D\tau\nu$.

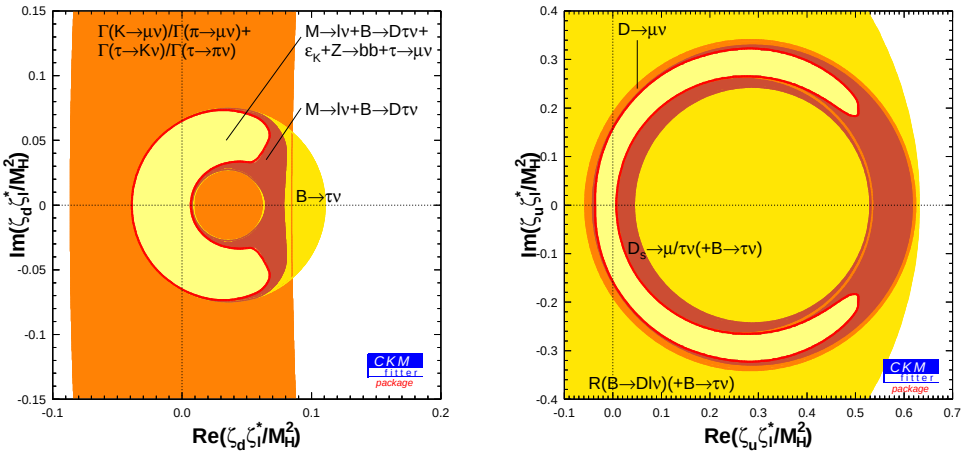

Figure 8: $\varsigma_d\varsigma_l^*/M_{H^\pm}^2$ *(left) and* $\varsigma_u\varsigma_l^*/M_{H^\pm}^2$ *(right) in the complex plane, in units of* GeV^{-2}*, constrained by leptonic and semileptonic decays. The inner yellow area shows the allowed region at 95% CL, in the case of* $\varsigma_d\varsigma_l^*/M_{H^\pm}^2$ *using additional information (see text).*

5. Loop-induced processes

For processes where new-physics contributions appear only through quantum loop effects, the situation becomes obviously more difficult, regarding not only the calculation but also the interpretation of the results. If the SM amplitude is also mediated only by loops, the relative importance of the charged-scalar contributions is expected to be higher, but this implies also a higher sensitivity to the framework in which the A2HDM is eventually to be embedded in. In the following we make the assumption that for the observables under discussion the dominant new-physics corrections are those generated by the charged scalar. Moreover, since no significant signal for new physics has been found up to now in flavour observables, we assume these effects to be subleading with respect to the SM contribution.

5.1 $\mathbf{Z \to b\bar{b}}$

The high-precision data collected at LEP and SLD has made it possible to accurately test the SM electroweak loop corrections at the Z scale, providing information on the Higgs mass and useful constraints on many new-physics scenarios. While most Z-peak observables are only sensitive to the gauge-boson selfenergies, the decay $Z \to b\bar{b}$ provides valuable information on fermionic vertex corrections induced by charged-current exchanges. Since $V_{tb} \approx 1$, those loop diagrams involving virtual top quarks generate quantum corrections to the $Zb\bar{b}$ vertex, which are absent in the $Zd\bar{d}$ and $Zs\bar{s}$ vertices. These corrections are enhanced by a factor m_t^2, allowing for a quite accurate determination of the top quark mass [112, 113]. The same arguments apply to the charged-scalar contributions present in the A2HDM, providing a sensitive probe of the corresponding $H^+\bar{t}b$ coupling. For very large values of $|\varsigma_d|$ this decay would also be sensitive to contributions from neutral scalars [114]; we don't consider this possibility here. However, given a not too small value for ς_l, (semi-)leptonic decays can be used to exclude that possibility.

Therefore, we assume the dominance of charged-scalar effects in the following, allowing only for $|\varsigma_d| \leq 50$. We disregard the information coming from the forward-backward polarization asymmetry A_b, because the scalar-exchange contributions to A_b are small compared to the present uncertainties.

It is convenient to normalize the $Z \to b\bar{b}$ decay width to the total hadronic width of the Z, because many QCD and electroweak corrections cancel in the ratio, amplifying the sensitivity to the wanted vertex contribution [113]. Within the A2HDM, this ratio can be written as [114, 115, 77]

$$R_b \equiv \frac{\Gamma(Z \to \bar{b}b)}{\Gamma(Z \to \text{hadrons})} = \left[1 + \frac{S_b}{s_b}\, C_b^{\text{QCD}}\right]^{-1}, \tag{5.1}$$

where

$$s_q = \left[(\bar{g}_b^L - \bar{g}_b^R)^2 + (\bar{g}_b^L + \bar{g}_b^R)^2\right] \left(1 + \frac{3\alpha}{4\pi}\, Q_q^2\right), \qquad S_b \equiv \sum_{q \neq b,t} s_q\,, \tag{5.2}$$

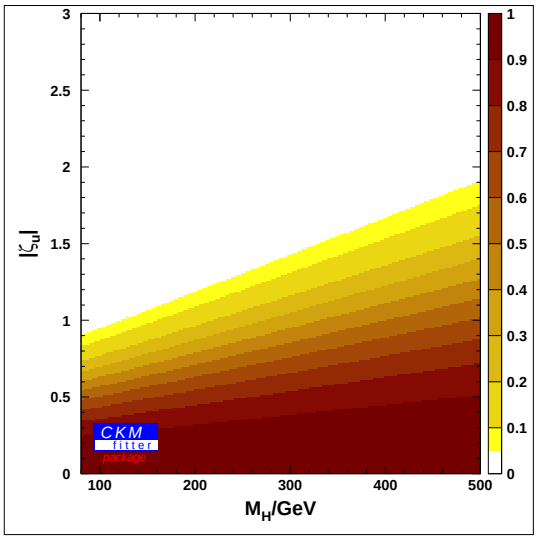

Figure 9: *Constraint from R_b in the $|\varsigma_u| - M_{H^\pm}$ plane ($M_{H^\pm}$ in GeV units), allowing for $|\varsigma_d| \leq 50$.*

with $C_b^{\rm QCD} = 1.0086$ being a factor including QCD corrections [116]. The A2HDM contributions are encoded through the effective left- and right-handed $Zb\bar{b}$-couplings:

$$\bar{g}_b^L = \bar{g}_{b,SM}^L + \frac{\sqrt{2}\,G_F M_W^2}{16\pi^2}\,\frac{m_t^2}{M_W^2}\,|\varsigma_u|^2\,\left[f_1(t_h) + \frac{\alpha_s}{3\pi}\,f_2(t_h)\right]\,, \tag{5.3}$$

$$\bar{g}_b^R = \bar{g}_{b,SM}^R - \frac{\sqrt{2}\,G_F M_W^2}{16\pi^2}\,\frac{m_b^2}{M_W^2}\,|\varsigma_d|^2\,\left[f_1(t_h) + \frac{\alpha_s}{3\pi}\,f_2(t_h)\right]\,, \tag{5.4}$$

where $t_h \equiv m_t^2/M_{H^\pm}^2$, $f_1(t_h) = [t_h^2 - t_h - t_h \log t_h]/(1-t_h)^2$ and the function $f_2(t_h)$ governing the NLO correction is given in [77]. If running quark masses $\bar{m}_t(M_Z)$ and $\bar{m}_b(M_Z)$ are used, this NLO QCD correction is small. The light-quark coupling contribution $S_b = 1.3214$ [76, 77] is not sensitive to the new-physics effects. The SM values of the couplings $\bar{g}_{b,SM}^{L,R}$, given in table 2, have been computed removing the $Z \to b\bar{b}$ information from the standard electroweak fit [76, 77].

In contrast to the leptonic and semileptonic constraints discussed before, here the parameters $|\varsigma_{u,d}|$ enter directly, allowing to bound them without information on $|\varsigma_l|$. The constraint resulting from the input values in tables 2 and 3 is shown in figure 9. The constraint is plotted in the $|\varsigma_u| - M_{H^\pm}$ plane, as obviously it is much weaker for $|\varsigma_d|$, due to the relative factor m_b/m_t. For large scalar masses, the constraint weakens as the effects start to decouple, reflected in $\lim_{t_h \to 0} f_{1,2}(t_h) = 0$. In the range of scalar masses considered, it leads to a 95% CL upper bound $|\varsigma_u| \leq 0.91$ (1.91), for $M_{H^\pm} = 80$ (500) GeV. The upper bound increases linearly with $M_{H^\pm}$, implying

$$\frac{|\varsigma_u|}{M_{H^\pm}} \;<\; 0.0024\ \text{GeV}^{-1} + \frac{0.72}{M_{H^\pm}} < 0.011\ \text{GeV}^{-1}\,, \tag{5.5}$$

where we have used the lower bound on the charged-scalar mass from LEP searches, $M_{H^\pm} > 78.6$ GeV (95% CL) [1, 81]. Combined with the limit on $|\varsigma_l/M_{H^\pm}|$ from leptonic τ decays,

this already constrains the combination $|\varsigma_u \varsigma_l^*|/M_{H^\pm}^2$ much stronger than the global fit to (semi)leptonic decays, leading to

$$\frac{|\varsigma_u \varsigma_l^*|}{M_{H^\pm}^2} \;<\; 0.005 \text{ GeV}^{-2}\,, \tag{5.6}$$

however only with the additional assumptions of $|\varsigma_d| \leq 50$ and charged-scalar effects dominating the new-physics contributions to R_b. The range allowed for $|\varsigma_d|$ in the fit does not influence the upper bound on $|\varsigma_u|$, apart from the exclusion of neutral-scalar effects, since both contributions can only lower the value for R_b and both are allowed to vanish in the fit. Therefore the upper limit stems from points with $|\varsigma_d| = 0$.

5.2 B^0-$\bar{B}^0$ mixing

The mixing of neutral B mesons is very sensitive to charged-scalar effects, as the leading contribution stems from top-quark loops, rendering the new-physics and SM contributions comparable. Besides the high precision of the measurement for the mass difference Δm_{B^0}, the B_s^0 mixing is especially interesting due to the observed tension in its phase [36, 65]. In the usual 2HDMs with a $\mathcal{Z}_2$ symmetry the scalar couplings are necessarily real, leading to a vanishing contribution to this phase. However, the complex Yukawa couplings $\varsigma_{u,d}$ of the A2HDM provide a potential new-physics contribution, which could account for the experimentally observed phase.

In the SM, the calculation is simplified by the fact that only one operator contributes, denoted $\mathcal{O}^{\text{VLL}}$ below. In the presence of a charged scalar, an enlarged effective Hamiltonian

$$\mathcal{H}_{\text{eff}}^{\Delta B=2} = \frac{G_F^2 M_W^2}{16\pi^2}\; (V_{td}^* V_{tb})^2 \sum_i C_i(\mu)\, \mathcal{O}_i \tag{5.7}$$

has to be considered, involving a basis of eight operators [117, 118, 119, 120]:

$$\begin{aligned}
\mathcal{O}^{\text{VLL,VRR}} &= \left(\bar{d}^\alpha \gamma_\mu \mathcal{P}_{L,R} b^\alpha\right)\left(\bar{d}^\beta \gamma^\mu \mathcal{P}_{L,R} b^\beta\right)\,,\\
\mathcal{O}_1^{\text{LR}} &= \left(\bar{d}^\alpha \gamma_\mu \mathcal{P}_L b^\alpha\right)\left(\bar{d}^\beta \gamma^\mu \mathcal{P}_R b^\beta\right)\,,\\
\mathcal{O}_2^{\text{LR}} &= \left(\bar{d}^\alpha \mathcal{P}_L b^\alpha\right)\left(\bar{d}^\beta \mathcal{P}_R b^\beta\right)\,,\\
\mathcal{O}_1^{\text{SLL,SRR}} &= \left(\bar{d}^\alpha \mathcal{P}_{L,R} b^\alpha\right)\left(\bar{d}^\beta \mathcal{P}_{L,R} b^\beta\right)\,,\\
\mathcal{O}_2^{\text{SLL,SRR}} &= \left(\bar{d}^\alpha \sigma_{\mu\nu} \mathcal{P}_{L,R} b^\alpha\right)\left(\bar{d}^\beta \sigma^{\mu\nu} \mathcal{P}_{L,R} b^\beta\right)\,,
\end{aligned} \tag{5.8}$$

with α, β being colour indices and $\sigma^{\mu\nu} = \frac{1}{2}[\gamma^\mu, \gamma^\nu]$. We have written the effective Hamiltonian relevant for B_d^0-$\bar{B}_d^0$ mixing; the mixing of B_s^0 mesons is described by the analogous expression, changing the label d to s everywhere.

We have performed the matching of the underlying A2HDM and the low-energy effective Hamiltonian at the scale $\mu_{tW} \sim M_W, m_t$. The resulting Wilson coefficients, given in the appendix, reproduce the SM result as well as the matching for the 2HDM in the limit $m_d \to 0$, given in [121]. As noted above, the contribution of the A2HDM to $C_{\text{VLL}}(\mu_{tW})$

is an $\mathcal{O}(1)$ effect. For that reason, we calculate this contribution at NLO, implementing the results of [121] within the A2HDM.[3] Owing to their chirality structure, the remaining Wilson coefficients are all suppressed by powers of the light-quark mass m_d (m_s in the B_s^0 case), except $C_{\rm SRR}^1$ which is proportional to m_b^2. Restricting the parameter ranges to $|\varsigma_u| \in [0,5]$ and $|\varsigma_d| \in [0,50]$, the ratio $|C_i(\mu_{tW})/C_{\rm VLL}(\mu_{tW})|$ is then below two percent for all operators apart from $\mathcal{O}_1^{\rm SRR}$. Since the matrix elements for the B^0 mixing do not contain the large (chiral) enhancement factors present in the kaon system, this allows us to restrict ourselves to two operators only. Moreover, the ratio $C_{\rm SRR}^1/C_{\rm VLL}$ is a small quantity (10% at most for $|\varsigma_d| \le 25$, still below 40% for $|\varsigma_d| = 50$) and therefore a leading-order estimate of the $\mathcal{O}_1^{\rm SRR}$ contribution is enough for our purposes, while the dominant $\mathcal{O}^{\rm VLL}$ contribution is included at NLO.

The strong $(m_s - m_d)/M_W$ suppression of SU(3)-breaking effects implies that, for the parameter ranges considered, the ratio $\Delta m_{B_s^0}/\Delta m_{B_d^0}$ is unaffected by charged-scalar contributions and can be used in the CKM fit. Note, however, that in the limit $|\varsigma_d| \gg 50$, $|\varsigma_u| \ll 1$, which corresponds to the large–tan β scenario in the type II model, the contribution from $\mathcal{O}^{\rm VRR}$ might become the dominant new-physics correction to B_s^0 mixing, but remains small compared to the SM one.

We use the ratio $\Delta m_{B_s^0}/\Delta m_{B_d^0}$ to determine the apex $(\bar\rho, \bar\eta)$ of the unitarity triangle, and bound the charged-scalar parameters with the B_s^0 mixing information. The resulting constraint from $\Delta m_{B_s^0}$ in the $M_{H^\pm}$– $|\varsigma_u|$ plane is shown in figure 10, using the scales $\mu_{tW} = m_t$ and $\mu_b = 4.2$ GeV. The error includes the variations in the CKM parameters, $f_{B_s^0}$, $\hat B_{B_s^0}$ and the experimental uncertainty. The leading $\mathcal{O}^{\rm VLL}$ contribution depends on $|\varsigma_u|^2$ only, while $C_{\rm SRR}^1$ is proportional to $\varsigma_u^*\varsigma_d = |\varsigma_u||\varsigma_d|e^{i\varphi}$, φ being the relative phase between the two Yukawa couplings. To determine the allowed region shown in figure 10, we have varied ς_d in the range $|\varsigma_d| < 50$ and $\varphi \in [0, 2\pi]$.

Interestingly, the dominant contribution to a possible phase shift in the mixing is also the one from $\mathcal{O}_1^{\rm SRR}$. The factor $M_W^4 D_0(m_t, M_{H^\pm})$ (see appendix) varies between zero and $\sim -3\%$ for scalar masses between 50 and 500 GeV, while $4m_b^2 m_t^4/M_W^6 \sim 10\%$. For relatively large values of the product $|\varsigma_u^*\varsigma_d|$ ($\gtrsim 20$) this factor can contribute sizeably to the B^0 mixing phase, as long as $M_{H^\pm}$ is relatively small. The sign of the shift is obviously not fixed, but depends on the sign of the relative Yukawa phase φ. As long as $|\varsigma_d|$ is not too large, the effect is the same in B_d^0 and B_s^0.

The D0 experiment has measured very recently [36] a like-sign dimuon charge asymmetry leading to $A_{sl}^b = -0.00957 \pm 0.00251 \pm 0.00146$, which differs by over three standard deviations from the SM prediction [122, 123]. The measurement includes contributions from B_d^0 and B_s^0 mesons, corresponding to $A_{sl}^b = (0.506 \pm 0.043)\, a_{sl}^d + (0.494 \pm 0.043)\, a_{sl}^s$, with $(q = d, s)$

$$a_{sl}^q \;=\; {\rm Im}\left(\frac{\Gamma_{12}^q}{M_{12}^q}\right) \;=\; \frac{|\Gamma_{12}^q|}{|M_{12}^q|}\,\sin\phi_q \;=\; \frac{\Delta\Gamma_{B_q^0}}{\Delta M_{B_q^0}}\,\tan\phi_q\,, \tag{5.9}$$

where $M_{12}^q - \frac{i}{2}\,\Gamma_{12}^q \equiv \langle B_q^0|\mathcal{H}_{\rm eff}^{\Delta B=2}|\bar B_q^0\rangle$. While this result needs certainly confirmation, we will explore some of its consequences for the parameters of the A2HDM in the follow-

[3] Note, that there are several smaller errors in that paper, most of which have been pointed out in [38].

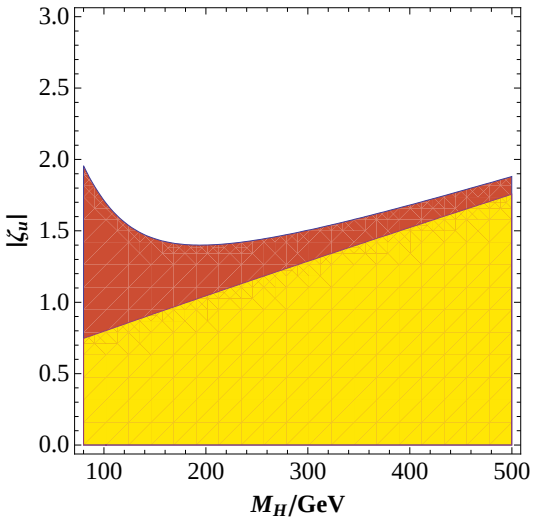

Figure 10: *The 95% CL constraint coming from $\Delta m_{B_s^0}$ in the $M_{H^\pm} - |\varsigma_u|$ plane for $|\varsigma_d| \in [0, 50]$, varying in addition the relative phase φ in $[0, 2\pi]$. The excluded area lies above the dark (red) region only. In yellow the allowed area for $\varsigma_d = 0$ is shown.*

ing. Using the current experimental value for the asymmetry in the B_d^0 system, $a_{sl}^d = -0.0047 \pm 0.0046$ [65], the measured value of $\Delta M_{B_s^0}$ and the SM prediction for $\Delta\Gamma_{B_s^0}$, the D0 asymmetry implies $\sin\phi_s = -2.7 \pm 1.4 \pm 1.6$, showing that the central value of this measurement is incompatible with the assumption of negligible influence of new physics on Γ_s^{12}, while the uncertainties are large enough to allow every value for the mixing phase at 2σ. Using in addition the direct measurement of a_{sl}^s through $B_s^0 \to \mu^+ D_s^- X$ decays by D0 [124], $a_{sl}^s = -0.0017 \pm 0.0091$, results in $\sin\phi_s = -1.7 \pm 1.1 \pm 1.0$. Note that (part of) the observed deviation may also be due to the possibility of bad convergence of the operator product expansion (OPE) [125, 126], related to the relatively low effective energy scale $m_b - 2m_c$. However, no signs for a breakdown were found in the above calculation. Note also that in [127] it has been argued that such a large value violates a "coherence bound" derived by demanding monotonicity of the Stokes vector in the B_s system. The possibility of NP influence on the rate as an explanation for this measurement has recently been discussed in [128, 129, 130]. The authors of [128] conclude, that most of the possible operators are strongly constrained by other processes (including the one discussed in [129]), leaving little space for an $\mathcal{O}(1)$ contribution to Γ_{12}^s.

Hints of a large ϕ_s value have been also obtained previously from $B_s^0 \to J/\psi\phi$ decays [131, 132, 133], where the extraction of the phase might however be influenced by contributions to the decay amplitude: in the SM, one of the reasons why this decay is "golden" is the fact, that the potentially relatively large penguin contributions have the same phase as the leading (colour-suppressed) tree amplitude, and therefore do not spoil the extraction of the mixing phase from the time-dependent CP asymmetry. However, this is no longer true in the A2HDM: the charged-scalar penguin contributions include terms similar to their leading SM counterparts, with an additional factor of $\varsigma_u^* \varsigma_d m_b m_t / M_{H^\pm}^2 \sim \mathcal{O}(1)$, thereby providing a second weak phase in the decay amplitude. Quantitatively assessing

the influence of these contributions would require a reliable calculation of the corresponding matrix elements, which is however not available; we are thus left with the possibility of a semi-quantitive analysis only, e.g. along the lines of [134], which we however do not consider here.

The SM predicts a very small positive value for ϕ_s and a much larger and negative result for ϕ_d. The theoretical values quoted in [122] are $\phi_s = 0.24^\circ \pm 0.08^\circ$ and $\phi_d = -5.2^\circ\, {}^{+1.5^\circ}_{-2.1^\circ}$.

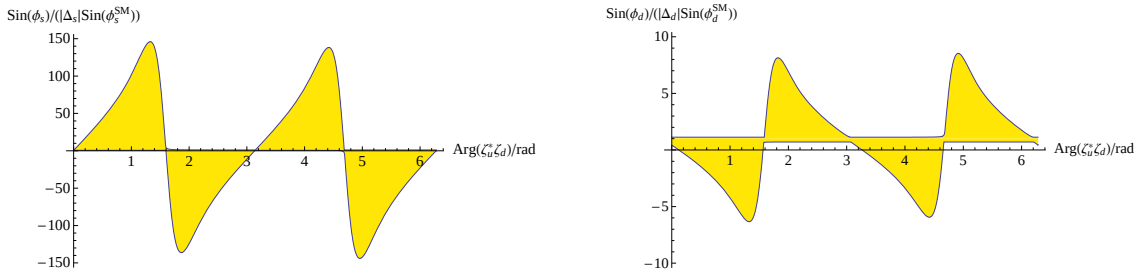

Figure 11: *Dependence of* $\sin\phi_q/(|\Delta_q|\sin\phi_q^{\rm SM})$ *on* $\varphi \equiv \arg(\varsigma_u^*\varsigma_d)$.

Assuming that the charged-scalar contributions are the only relevant new-physics effects, we can analyze the possibility to accommodate a large ϕ_s phase within the A2HDM. In figure 11 we plot the allowed range for $\sin\phi_q/(|\Delta_q|\sin\phi_q^{\rm SM})$, where $\Delta_q \equiv M_{12}^q/M_{12}^{q,{\rm SM}}$, as a function of the relative Yukawa phase $\varphi \equiv \arg(\varsigma_u^*\varsigma_d)$. The other scalar parameters have been varied in the ranges $|\varsigma_d| \in [0, 50]$, $M_{H^\pm} \in [80, 500]$ GeV, and $|\varsigma_u|$ according to the allowed range from $\epsilon_K, Z \to \bar{b}b$, which includes only values for $(|\varsigma_u|, M_{H^\pm})$ which lead to acceptable values for $\Delta m_{s,d}$. While it is indeed possible to obtain a large value of ϕ_s, the predicted equality of Δ_s and Δ_d implies a strong anti-correlation of $\sin\phi_d/(|\Delta_d|\sin\phi_d^{\rm SM})$ and $\sin\phi_s/(|\Delta_s|\sin\phi_s^{\rm SM})$, due to the different sign (and size) of $\phi_d^{\rm SM}$ and $\phi_s^{\rm SM}$. This leads to a prediction for the sign of a_{sl}^d, which could be verified/falsified, once higher experimental precision is achieved. As can be seen, the preferred negative sign for the a_{sl}^s asymmetry implies $\varphi \in [\pi/2, \pi], [3\pi/2, 2\pi]$, and for possible large values the Yukawa phase should not be close to $0, \pi$ (obviously).

Figure 12 shows the dependence of $\sin\phi_s/(|\Delta_s|\sin\phi_s^{\rm SM})$ with $|\varsigma_d|$ (left) and $M_{H^\pm}$ (right), varying the remaining parameters within their allowed ranges. If large values for the a_{sl}^s asymmetry are confirmed (within the physical range $|\sin\phi_s| \leq 1$), this would point towards large values of $|\varsigma_d|$ and small charged scalar masses. Finally we show in figure 13 the plots from figure 11 again, restricting the product $|\varsigma_u\varsigma_d^*| \leq 20$ (see section 5.4). The corresponding maximal asymmetry is correspondingly smaller, but still relative factors up to ~ 60 are allowed for B_s with respect to the SM.

Additional contributions to ϕ_s could be induced by neutral scalar exchanges, through the effective FCNC operator in Eq.(2.13) appearing at the one-loop level. Also, a sizable Yukawa phase $\varphi \equiv \arg(\varsigma_u^*\varsigma_d)$ could generate observable signals in other CP-violating observables not yet included in our analysis. A detailed discussion of these effects and their corresponding constraints on the model parameters is postponed to future work.

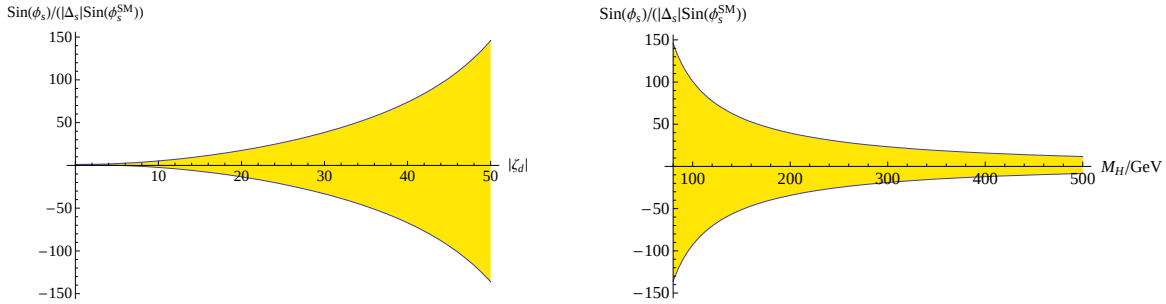

Figure 12: *Dependence of* $\sin\phi_s/(|\Delta_s|\sin\phi_s^{\rm SM})$ *on* $|\varsigma_d|$ *(left) and* $M_{H^\pm}$ *(right).*

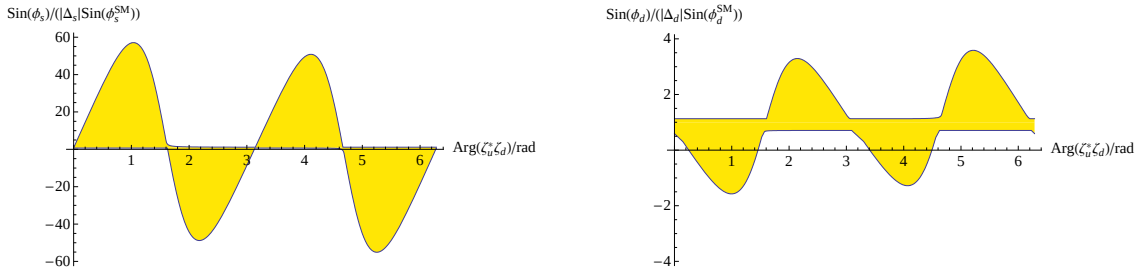

Figure 13: *Dependence of* $\sin\phi_q/(|\Delta_q|\sin\phi_q^{\rm SM})$ *on* $\varphi\equiv\arg(\varsigma_u^*\varsigma_d)$*, constraining* $|\varsigma_u\varsigma_d^*|\le 20$*.*

5.3 $\mathbf{K^0}$-$\mathbf{\bar K^0}$ mixing: $\epsilon_{\mathbf{K}}$

The $\Delta S=2$ effective Hamiltonian is described by the same basis of four-quark operators given in (5.8), changing the flavour b to s everywhere. However, the small light-quark masses m_d and m_s suppress now the contributions from all operators except $\mathcal{O}^{\rm VLL}$. Another difference with respect to B^0 mixing is that, owing to the different CKM factors, one needs to consider the virtual contributions from top and charm quark exchanges within the box diagrams:

$$\mathcal{H}_{\rm eff}^{\Delta S=2} \;=\; \frac{G_F^2 M_W^2}{16\pi^2}\,\left\{\lambda_t^2\, C_{\rm VLL}^{tt}(\mu)+\lambda_c^2\, C_{\rm VLL}^{cc}(\mu)+2\lambda_t\lambda_c\, C_{\rm VLL}^{ct}(\mu)\right\}\,\left(\bar d\gamma_\mu\mathcal{P}_L s\right)\left(\bar d\gamma^\mu\mathcal{P}_L s\right)\,. \tag{5.10}$$

Since $\lambda_t\equiv V_{td}^*V_{ts}\sim A^2\lambda^5$ while $\lambda_t\equiv V_{cd}^*V_{cs}\sim\lambda$, in spite of the m_c^2/m_t^2 relative suppression, the charm loop gives the dominant short-distance contribution to Δm_K. There are in addition large corrections from long-distance physics, which make it difficult to extract from Δm_K useful constraints on the new-physics amplitude.

More interesting is the CP-violating parameter ϵ_K, which can be written in the form

$$\epsilon_K \;=\; \frac{\kappa_\epsilon\, e^{i\phi_\epsilon}}{\sqrt{2}}\,\frac{{\rm Im}(M_{12})}{\Delta m_K}\,, \tag{5.11}$$

where $\kappa_\epsilon=0.94\pm0.02$ takes into account small long-distance corrections [135, 78]. The top and charm contributions are now weighted by less hierarchical CKM factors ${\rm Im}(\lambda_t^2)\sim$

$\lambda^4 \mathrm{Im}(\lambda_c \lambda_t) \sim \lambda^4 \mathrm{Im}(\lambda_c^2)$; the mass hierarchy compensates for this, implying that the top quark gives the most important contribution to ϵ_K.

The relevant Wilson coefficients $C_{\mathrm{VLL}}^{qq'}$, containing the SM and new-physics contributions, are given in the appendix. The corrections induced by the charged scalar are proportional to $|\varsigma_u|^2$ and $|\varsigma_u|^4$. All contributions from the coupling ς_d are absent in the limit $m_{d,s} = 0$. The matrix element $\langle K^0 | \mathcal{H}_{\mathrm{eff}}^{\Delta S=2} | \bar{K}^0 \rangle$ is parametrized through the hadronic

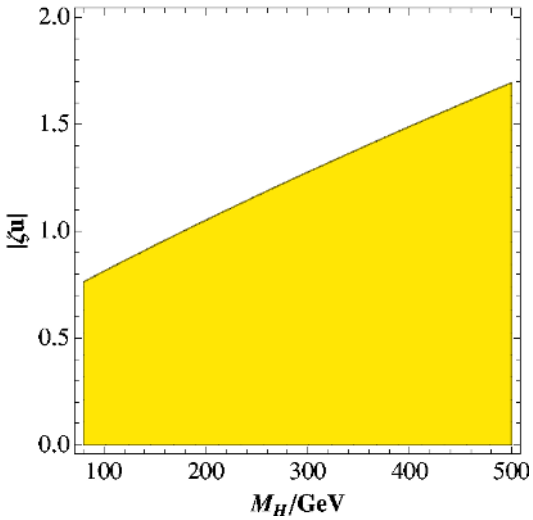

Figure 14: *95% CL constraints from ϵ_K.*

quantity $f_K^2 \hat{B}_K$. We use the numerical values of f_K/f_π and $\hat{B}_K$, given in table 2, together with the phenomenological determination of the pion decay constant from $\Gamma(\pi^+ \to \mu^+ \nu_\mu)$, $f_\pi = 130.4 \pm 0.04 \pm 0.2$ MeV [66]. Figure 14 shows the constraint obtained from ϵ_K in the plane $M_{H^\pm}$ – $|\varsigma_u|$. It is very similar to the one extracted from $Z \to b\bar{b}$, and even slightly stronger.

5.4 $\bar{\mathbf{B}} \to \mathbf{X_s \gamma}$

The radiative decay $\bar{B} \to X_s \gamma$ has been calculated at NNLO in the SM, leading to the prediction $\mathrm{Br}(\bar{B} \to X_s \gamma)_{\mathrm{SM}} = (3.15 \pm 0.23) \times 10^{-4}$ [136]. In the 2HDM the decay amplitude is known at NLO [137, 138, 77, 139]. Following the steps given in [140], one can express the branching ratio as

$$\mathrm{Br}(\bar{B} \to X_s \gamma)_{E_\gamma > E_0} \;=\; \mathrm{Br}(\bar{B} \to X_c e \bar{\nu})_{\mathrm{exp}} \left| \frac{V_{ts}^* V_{tb}}{V_{cb}} \right|^2 \frac{6\alpha}{\pi C_B} \left[P(E_0) + N(E_0) \right] , \qquad (5.12)$$

where the phase-space factor $C_B = |V_{ub}/V_{cb}|^2 \Gamma(\bar{B} \to X_c e \bar{\nu}) / \Gamma(\bar{B} \to X_u e \bar{\nu}) = 0.580 \pm 0.016$ [141] accounts for the m_c dependence of $\mathrm{Br}(\bar{B} \to X_c e \bar{\nu})$. Normalizing the result with the $\bar{B} \to X_c e \bar{\nu}$ transition, cancels the leading non-perturbative corrections of order Λ^2/m_b^2 and minimizes many sources of uncertainties, such as those generated by the CKM quark-mixing factors, the dependence on m_b^5 and the sensitivity to m_c. The subleading non-perturbative contributions are contained in $N(E_0)$, which includes corrections of $\mathcal{O}(\Lambda^2/m_c^2)$

[142], $\mathcal{O}(\Lambda^3/m_b^3)$, $\mathcal{O}(\Lambda^3/m_b m_c^2)$ [143] and $\mathcal{O}(\alpha_s\Lambda^2/(m_b-2E_0)^2)$ [144]. The relevant combination of CKM factors is given by

$$\left|\frac{V_{ts}^* V_{tb}}{V_{cb}}\right|^2 \;=\; 1+\lambda^2(2\bar\rho-1)+\lambda^4(\bar\rho^2+\bar\eta^2-A^2)+\mathcal{O}(\lambda^6) \;=\; 0.963\pm 0.002\pm 0.005\,, \quad (5.13)$$

where the sensitivity to the apex $(\bar\rho,\bar\eta)$ of the unitarity triangle is suppressed by two powers of λ.

For $m_s = 0$ the effective low-energy operator basis remains the same as in the SM. The modifications induced by new-physics contributions appear only in the Wilson coefficients, which are included in the perturbative part $P(E_0)$:

$$C_i^{\rm eff}(\mu_W) = C_{i,SM} + |\varsigma_u|^2\, C_{i,uu} - (\varsigma_u^*\varsigma_d\ )\, C_{i,ud}\,, \quad (5.14)$$

where $\varsigma_u^*\varsigma_d\ = |\varsigma_u||\varsigma_d|e^{i\varphi}$, φ being the relative phase. The virtual top-quark contributions dominate the coefficients $C_{i,uu}$ and $C_{i,ud}$; their explicit expressions as a function of m_t can be found in [77]. Depending on the value of the phase φ, the combined effect of the two terms $C_{i,uu}$ and $C_{i,ud}$ can be rather different. For instance, these two terms tend to cancel each other in the type I model where $\varphi = 0$, while in the type II version with $\varphi = \pi$ they add constructively.

Since the new-physics contribution is only calculated up to NLO, terms in the branching ratio of $\mathcal{O}(\alpha_s^2)$ coming from the square of the 2HDM amplitude are neglected consistently. In some regions of the parameter space, leading to large new-physics effects of opposite sign to the SM amplitude, the cancellations between the two contributions enhance the sensitivity to higher-order QCD corrections, generating in some cases unphysical results (for instance in the type I model at small values of $\tan\beta$) [138]. Fortunately, the most problematic region (large values of $|\varsigma_u|$) is already excluded by the constraints from $Z\to\bar b b$ and $\Delta m_{B_s^0}$. The inclusion of the SM NNLO contributions substantially improves the reliability of the theoretical predictions.

To extract the information on the A2HDM couplings, we take into account the latest experimental values, given in table 3, and use the same renormalization scales as in [140] ($\mu_0 = 160$ GeV, $\mu_b = 2.5$ GeV and $\mu_c = 1.5$ GeV as central values and the same ranges of variation). We follow again the RFit approach, adding the theoretical uncertainty linearly to the systematic error. The resulting constraints on $|\varsigma_u|$ and $|\varsigma_d|$ are shown in figure 15, varying the charged-scalar mass in the range $M_{H^\pm}\in[80,500]$ GeV. The white areas are excluded at 95% CL. In the left plot, the phase φ has been scanned in the whole range from 0 to 2π; the resulting constraints are not very strong because a destructive interference between the two terms in (5.14) can be adjusted through the relative phase. In the range $|\varsigma_u|<2$, one finds roughly $|\varsigma_d||\varsigma_u|<20$ (95% CL). More stringent bounds are obtained at fixed values of the relative phase. This is shown in the right plot, where ς_u and ς_d have been assumed to be real (i.e. $\varphi = 0$ or π). In that case, couplings of different sign are excluded, except at very small values, while a broad region of large equal-sign couplings is allowed, reflecting again the possibility of a destructive interference.

The sensitivity to the charged-scalar mass is illustrated in figure 16, which shows the constraints on $|\varsigma_d|$ versus $M_{H^\pm}$ for fixed values of $\varsigma_u = 0.5$ (left) and $\varsigma_u = 1.5$ (right). Again,

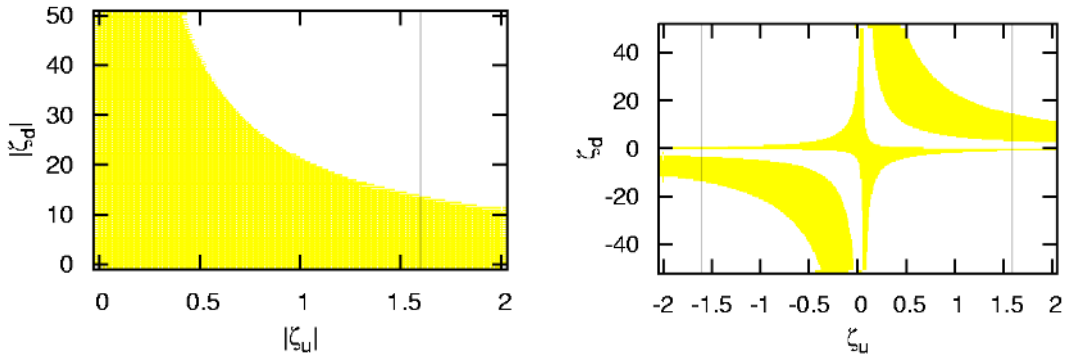

Figure 15: *Constraints on ς_u and ς_d from $\bar{B} \to X_s\gamma$, taking $M_{H^\pm} \in [80, 500]$ GeV. The white areas are excluded at 95% CL. The black line corresponds to the upper limit from $\epsilon_K, Z \to \bar{b}b$ on $|\varsigma_u|$. In the left panel, the relative phase has been varied in the range $\varphi \in [0, 2\pi]$. The right panel assumes real couplings.*

in the upper plots the relative phase has been varied in the whole range $\varphi \in [0, 2\pi]$, while the lower plots assume real couplings. Figure 17 shows the constraints on the $|\varsigma_u| - M_{H^\pm}$ plane, for $\varsigma_d = 0$. Finally, in figure 18 we show the constraints obtained for fixed values of the charged-scalar mass, assuming ς_u and ς_d to be real. We reproduce in this case the qualitative behaviour obtained in [42].

We observe that for small values of $|\varsigma_u|$ no constraint on ς_d is obtained, because in the limit $|\varsigma_u| \to 0$ the SM is recovered, which is compatible with the data. With growing $|\varsigma_u|$ a bound on $|\varsigma_d|$ emerges, corresponding to $|\varsigma_u\varsigma_d| \lesssim 20$. For $\varsigma_d = 0$ on the other hand, a limit of $|\varsigma_u| \lesssim 3$ can be observed for large scalar masses around 500 GeV, strengthening to $|\varsigma_u| \lesssim 1.3$ for smaller values of $M_{H^\pm}$. The overall constraint is relatively weak compared to the strong bound on $M_{H^\pm}$ obtained in the type II 2HDM, due to the correlation $\varsigma_u\varsigma_d = -1$. However, it can be seen from the plots with vanishing phase and/or a fixed value for $|\varsigma_{d,u}|$ that this strength is recovered, once some parameters are constrained independently. Comparing the plots with complex input parameters to their real counterparts, we observe that the effect of the relative phase is mainly to extend the allowed bands in a way that the excluded space between them is rendered allowed, too.

We have also analyzed the CP rate asymmetry, defined as

$$a_{CP} = \frac{BR(\bar{B} \to X_s\gamma) - BR(B \to X_{\bar{s}}\gamma)}{BR(\bar{B} \to X_s\gamma) + BR(B \to X_{\bar{s}}\gamma)}, \tag{5.15}$$

which is predicted to be tiny in the SM. Once the constraints from the branching ratio are implemented in the A2HDM, the predicted asymmetry is smaller than the present experimental bounds. Thus, one does not obtain further constraints on the model parameters. A sizable Yukawa phase φ could generate values of the CP-asymmetry large enough to be relevant for future high-precision experimental analyses. However, a NNLO analysis of the theoretical prediction appears to be needed to reduce the presently large theoretical uncertainties and fully exploit such a measurement.

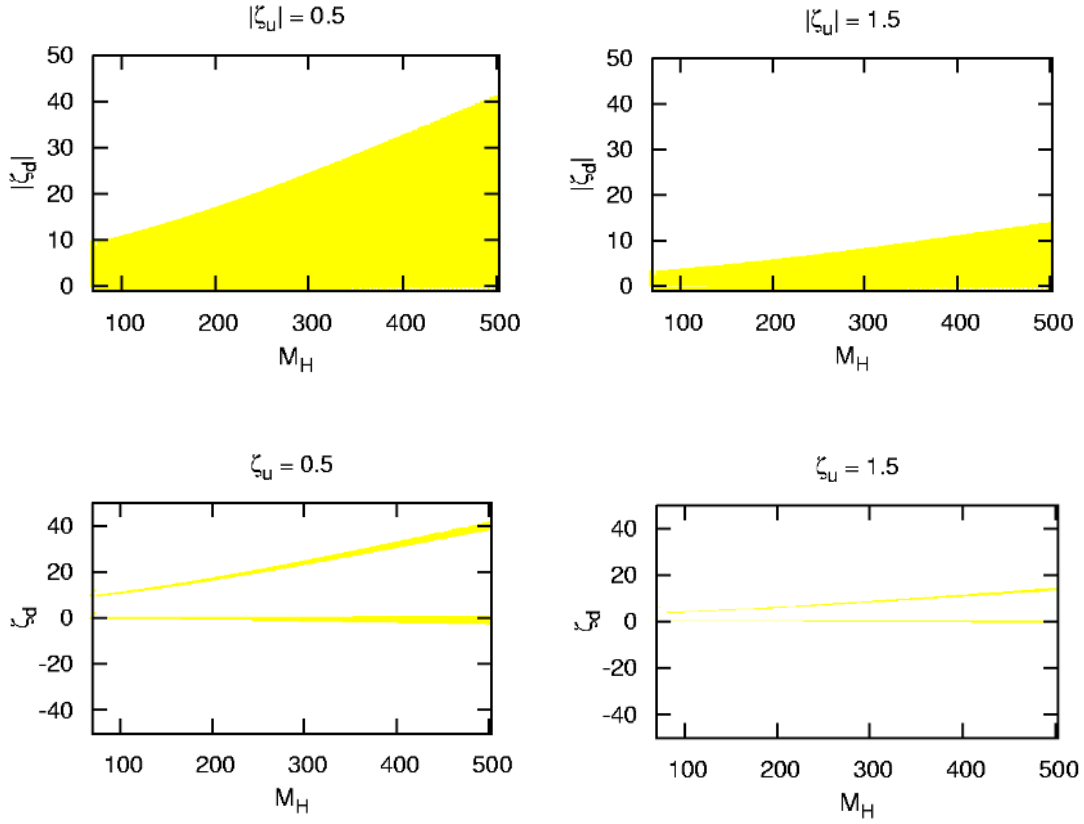

Figure 16: *Constraints on $|\varsigma_d|$ versus $M_{H^\pm}$ (in GeV) from $\bar{B} \to X_s\gamma$, for $\varsigma_u = 0.5$ (left) and $\varsigma_u = 1.5$ (right). The white areas are excluded at 95% CL. In the upper panels, the phase has been varied in the range $\varphi \in [0, 2\pi]$. The lower panels assume real couplings.*

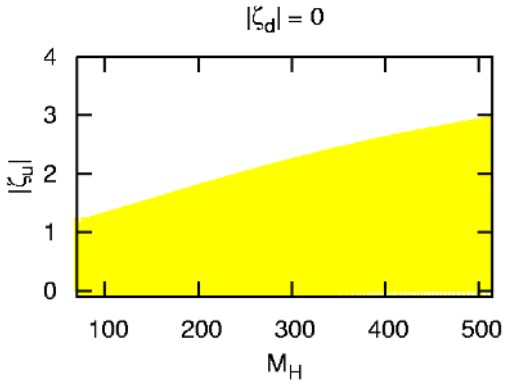

Figure 17: *Constraints on $|\varsigma_u|$ versus $M_{H^\pm}$ (in GeV) from $\bar{B} \to X_s\gamma$, for $\varsigma_d = 0$. The white area is excluded at 95% CL.*

6. Discussion

Imposing natural flavour conservation through discrete $\mathcal{Z}_2$ symmetries, one finds that the

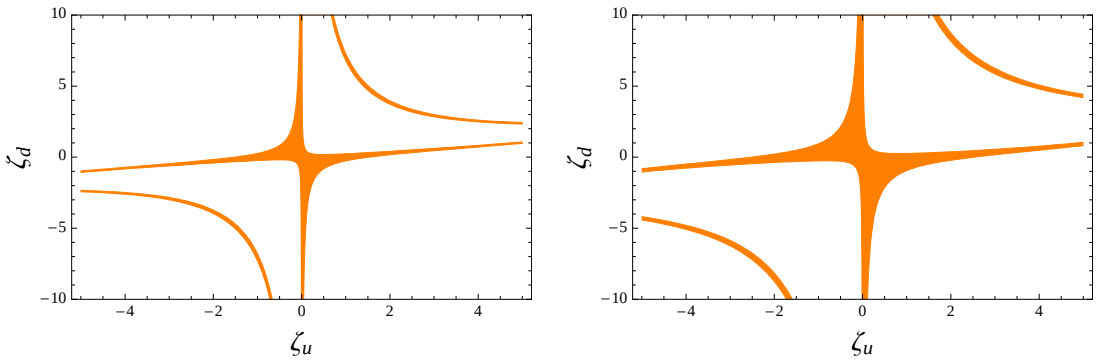

Figure 18: *Constraints on ς_d versus ς_u (95% CL) from $\bar{B} \to X_s\gamma$, assuming real couplings and taking $M_{H^\pm} = 150$ GeV (left) and $M_{H^\pm} = 400$ GeV (right).*

CKM phase is the only source of CP violation in the resulting 2HDMs. During the last thirty years, it has been common lore to assume that this is a more general fact, i.e. that the absence of tree-level FCNCs implies the absence of additional phases beyond the CKM one. The A2HDM provides an explicit counter-example, where FCNC couplings are absent at the Lagrangian level, while additional unconstrained complex phases generate new sources of CP violation. Since all Yukawa couplings are proportional to fermion masses, the A2HDM gives rise to an interesting hierarchy of FCNC effects, avoiding the stringent experimental constraints for light-quark systems and predicting at the same time interesting signals in heavy-quark transitions. The flavour-blind phases present in the model open a very interesting phenomenology which is worth to be investigated. The built-in flavour symmetries protect very efficiently the A2HDM from unwanted FCNC effects generated through quantum corrections. At the one-loop level the only allowed FCNC local structures are the two operators in (2.13), which could have very interesting (and computable) implications for B_s^0 mixing.

Besides the fermion masses and mixings, the charged-scalar couplings of the A2HDM are fully characterized by three complex parameters ς_f. In the previous sections, we have analyzed the impact of the $H^\pm$ contribution to different observables, where it is expected to be the dominant new-physics effect. Using conservatively estimated hadronic parameters and up-to-date data, we have inferred the present constraints on the new-physics parameters involved in these processes.

Leptonic tau decays provide a direct bound on the leptonic Yukawa coupling: $|\varsigma_l|/M_{H^\pm} \leq 0.40\ \text{GeV}^{-1}$ (95% CL). From semileptonic processes constraints on the products $\varsigma_l^*\varsigma_u/M_{H^\pm}^2$ and $\varsigma_l^*\varsigma_d/M_{H^\pm}^2$ are derived. The leptonic decays of heavy-light mesons allow us to disentangle the effects from ς_u and ς_d. Thus, from $B \to \tau\nu$ we derive an annular constraint in the complex plane $\varsigma_l^*\varsigma_d/M_{H^\pm}^2$ (figure 1a), implying the absolute bound $|\varsigma_l^*\varsigma_d/M_{H^\pm}^2| < 0.108\ \text{GeV}^{-2}$ (95% CL). For real Yukawa couplings there is a two-fold sign ambiguity generating two possible solutions, the expected one around $\Delta_{ij} = 0$ (the SM amplitude dominates) and its mirror around $\Delta_{ij} = 2$, corresponding to a new-physics contribution twice as large as the SM one and of opposite sign. The real solutions are

$\varsigma_l^*\varsigma_d/M_{H^\pm}^2 \in [-0.036, 0.008]$ GeV^{-2} and $[0.065, 0.108]$ GeV^{-2}.

Similar, but slightly weaker constraints on $\varsigma_l^*\varsigma_u/M_{H^\pm}^2$ are obtained from the decays $D \to \mu\nu$ (figure 1b) and $D_s \to (\tau, \mu)\nu$ (figure 2); in the last case the bounds from $B \to \tau\nu$ are used to get rid of the small ς_d contamination proportional to the strange quark mass. The resulting absolute bound $|\varsigma_l^*\varsigma_u/M_{H^\pm}^2| < 0.6$ GeV^{-2} (95% CL) is rather weak, but the upper limit corresponds to a new-physics contribution twice as large as the SM one, a very unlikely situation. The annular form of these constraints results in much stronger limits, once this possibility is excluded by other processes. For real Yukawa couplings, one finds $\varsigma_l^*\varsigma_u/M_{H^\pm}^2 \in [-0.005, 0.037]$ GeV^{-2} or $[0.511, 0.535]$ GeV^{-2}, at 95% CL.

Owing to the quark-mass suppression, the absolute constraints obtained from leptonic decays of light mesons (figure 4) are obviously much weaker. However, the excellent experimental precision achieved in π and K decays implies a narrow allowed annular region. For real Yukawa couplings this translates into quite stringent bounds: $\varsigma_l^*\varsigma_d/M_{H^\pm}^2 \in [-0.07, 0.07]$ GeV^{-2} or $[8.14, 8.28]$ GeV^{-2} (95% CL). The uncertainties are dominated by the present theoretical knowledge of the ratio f_K/f_π.

Independent information is obtained from the semileptonic decays of pseudoscalar mesons, through the scalar form-factor contribution. One needs, however, to disentangle the dominant vector form-factor amplitude, which does not contain any charged-scalar effect and is correlated with the usual measurement of the corresponding CKM mixing factor. The present constraints from the ratio $\mathrm{Br}(B \to D\tau\nu_\tau)/\mathrm{Br}(B \to De\nu_e)$, shown in figures 5 and 6, are not very strong by themselves, but allow in combination with other processes the exclusion of the second real solutions in the $\varsigma_{u,d}\varsigma_l^*/M_{H^\pm}^2$ planes. A future measurement of the differential distribution in $B \to D\tau\nu_\tau$ would obviously increase the sensitivity to the scalar contribution. In spite of the strange-mass suppression, the much higher experimental accuracy achieved in the analysis of $K \to \pi l\nu$ decays allows to derive the bound $\mathrm{Re}(\varsigma_l^*\varsigma_d/M_{H^\pm}^2) \in [-0.16, 0.30]$ GeV^{-2} (95% CL). This already excludes the second real solution (a scalar amplitude larger than the SM one) obtained from $K_{\mu 2}/\pi_{\mu 2}$.

Combining the information from all leptonic and semileptonic decays analyzed, one gets the constraints shown in figure 8.

The flavour-conserving decay $Z \to b\bar{b}$ provides a very stringent constraint on $|\varsigma_u|$. Since $V_{tb} \approx 1$, the one-loop contributions involving virtual top quarks completely dominate both the SM ($W^\pm$) and the new-physics ($H^\pm$) radiative corrections. In contrast to leptonic and semileptonic processes, where the charged-scalar effects are necessarily proportional to ς_l, the $Z \to b\bar{b}$ amplitude gives direct access to ς_u and ς_d. Owing to the relative factor m_b/m_t which suppresses the ς_d contribution, one gets finally the constraints on $|\varsigma_u|$ shown in figure 9 (assuming $|\varsigma_d| \leq 50$). At 95% CL, we obtain $|\varsigma_u| < 0.91$ (1.91), for $M_{H^\pm} = 80$ (500) GeV. The upper bound increases linearly with $M_{H^\pm}$, implying $|\varsigma_u|/M_{H^\pm} < 0.0024$ GeV$^{-1} + \frac{0.72}{M_{H^\pm}} < 0.011$ GeV^{-1}, where we have used the LEP lower bound on the charged-scalar mass $M_{H^\pm} > 78.6$ GeV (95% CL) [1, 81]. Together with the tau-decay constraint on $|\varsigma_l|/M_{H^\pm}$, this gives the limit $|\varsigma_u\varsigma_l^*|/M_{H^\pm}^2 < 0.005$ GeV^{-2}, which is much stronger than the information extracted from the global fit to leptonic and semileptonic decays.

Quite similar information can be extracted from B^0 mixing, which is also dominated

by one-loop contributions involving virtual top quarks. The smallness of the m_s/M_W ratio implies that SU(3)-breaking corrections are negligible; therefore, the charged-scalar contributions cancel in the ratio $\Delta m_{B_s^0}/\Delta m_{B_d^0}$, which can be used in the CKM fit. Only two $\Delta B = 2$ four-quark operators are numerically relevant; the one generating the leading SM amplitude gets new-physics contributions proportional to $|\varsigma_u|^{2,4}$, while the other operator generates subleading corrections proportional to $(\varsigma_u^*\varsigma_d)^{1,2} m_b^2/M_W^2$. Scanning the parameter ranges $|\varsigma_d| < 50$ and $\varphi \in [0, 2\pi]$, where φ is the relative phase between ς_u and ς_d, the measured B_s^0 mixing amplitude implies the constraints shown in figure 10, in the plane $M_{H^\pm}$– $|\varsigma_u|$. At 95% CL, one gets $|\varsigma_u| < 0.00279\, M_{H^\pm} + 0.27 + 117/M_{H^\pm}$, for $M_{H^\pm} \in [80, 500]$, in GeV units.

The charged-scalar contribution could accommodate a large B_s^0 mixing phase, without spoiling the agreement in the B_d system, although it is not possible to reach a value as large as hinted at by the present D0 central value, which is however at odds with the rate difference being unaffected by new physics (unless the calculation of the rate difference is affected by problems regarding the OPE). If confirmed, a large phase ϕ_s would point towards large values of $|\varsigma_d|$, small charged-scalar masses and a sizable Yukawa phase φ. The preferred negative sign for the a_{sl}^s asymmetry would require $\varphi \in [\pi/2, \pi], [3\pi/2, 2\pi]$. Additional contributions to ϕ_s could be induced by neutral scalar exchanges, through the effective FCNC operator in Eq.(2.13) appearing at the one-loop level. Large Yukawa phases could be constrained by other CP-violating observables not yet included in our analysis. A detailed discussion of these effects is postponed to future work.

The observable ϵ_K leads again to a similar constraint, even slightly more restrictive than the ones from B^0 mixing and $Z \to \bar{b}b$. Although CP violating, this observable is insensitive to the new-physics phases, as the relevant contributions involve $|\varsigma_u|$, only. We obtain at 95% CL $|\varsigma_u| \leq 0.560 + 2.647\, 10^{-3} M_{H^\pm} - 1.049\, 10^{-6} M_{H^\pm}^2 + 6.153\, 10^{-10} M_{H^\pm}^3$ in units of GeV.

The radiative decay $\bar{B} \to X_s\gamma$ provides another important source of information. There are two different charged-scalar contributions, proportional again to $|\varsigma_u|^2$ and $\varsigma_u^*\varsigma_d$, but in this case the two have similar sizes. Their combined effect can be quite different depending on the value of the relative phase φ. This results in rather weak limits because a destructive interference can be adjusted through this phase. The resulting constraints on $|\varsigma_u|$ and $|\varsigma_d|$ are shown in figure 15, varying the charged-scalar mass in the range $M_{H^\pm} \in [80, 500]$ GeV. Scanning the phase φ in the whole range from 0 to 2π, and imposing $|\varsigma_u| < 3$, one finds roughly $|\varsigma_d||\varsigma_u| < 20$ (95% CL). Much stronger bounds are obtained at fixed values of the relative phase. Assuming real values of ς_u and ς_d (i.e. $\varphi = 0$ or π), one finds that couplings of different sign are excluded, except at very small values, while a broad region of large equal-sign couplings is allowed, reflecting again the possibility of a destructive interference. Figures 16, 17 and 18 show the sensitivity of the $\bar{B} \to X_s\gamma$ constraints to the different unknown parameters: $M_{H^\pm}$, $|\varsigma_u|$, $|\varsigma_d|$ and φ.

The constraints discussed so far apply to the general A2HDM framework, with three arbitrary complex parameters ς_f. The limits become of course much stronger in particular models where these parameters are correlated. Figures 19 show the combined constraints

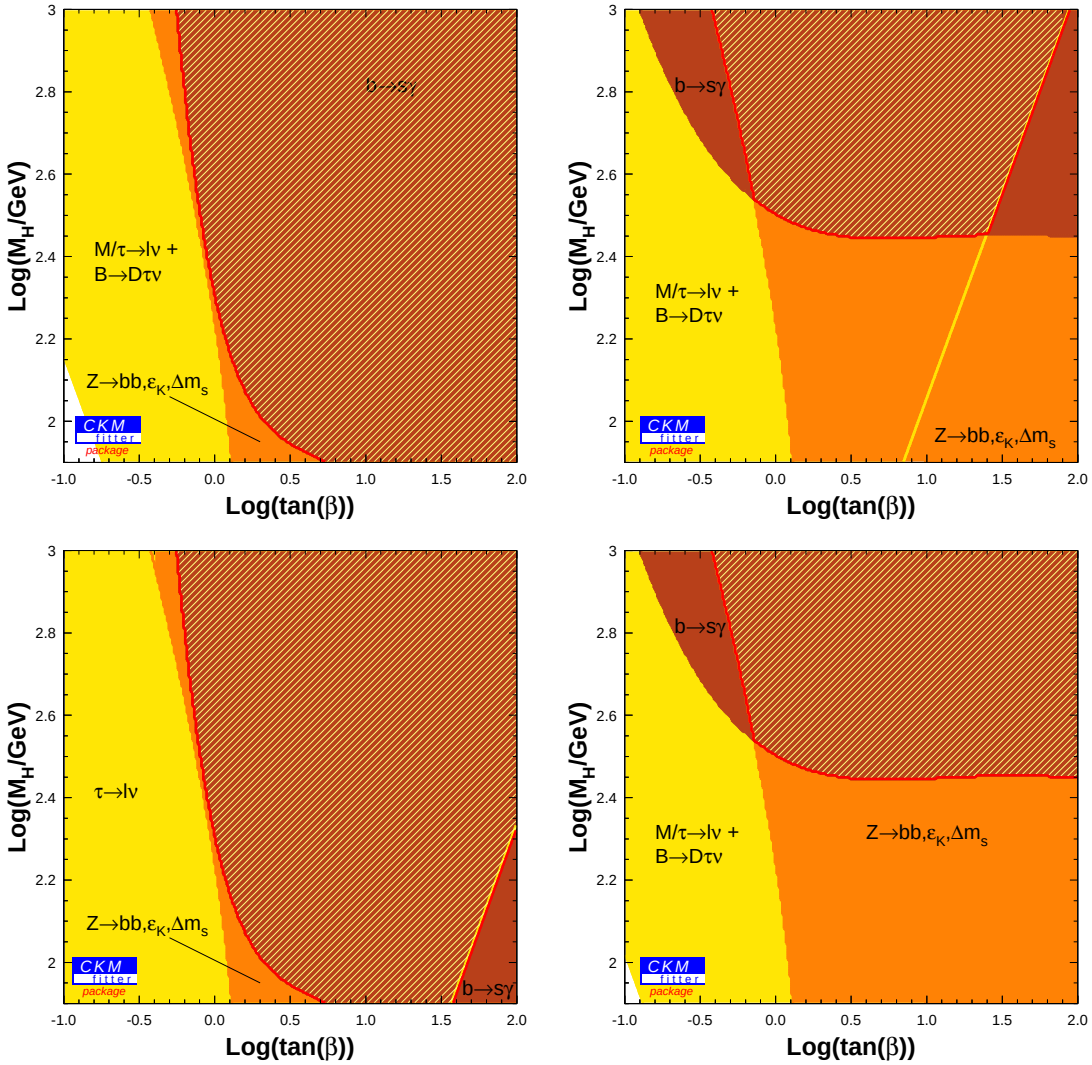

Figure 19: *Constraints on $M_{H^\pm}$ (in GeV) versus* $\tan\beta$ *(95% CL), in the 2HDM models of types I (upper-left), II (upper-right), X (lower-left) and Y (lower-right).*

on the $\tan\beta$–$M_{H^\pm}$ plane for the different $\mathcal{Z}_2$ models. The bounds from $Z \to b\bar{b}$, ϵ_K, $\Delta m_{B_s^0}$ and $\bar{B} \to X_s\gamma$ are obviously identical for the models of type I and X and also for type II and Y. In the type I/X case, $\varsigma_u^2 = \varsigma_d^2 = \varsigma_u\varsigma_d = \cot^2\beta$ and the scalar amplitudes grow for decreasing values of $\tan\beta$. For type II/Y, this behaviour is only observed in the ς_u^2 term, while $\varsigma_d^2 = \tan^2\beta$ and $\varsigma_u\varsigma_d = -1$; the decay $\bar{B} \to X_s\gamma$ provides then a very strong lower bound on the scalar mass, $M_{H^\pm} > 277$ GeV (95% CL), due to the constructive interference of the two contributing amplitudes. The ς_l coupling gives rise to different constraints from leptonic and semileptonic decays in each of the four models. Our results agree with the qualitative behaviour found in previous analyses [14, 38, 39, 40, 41, 42, 136, 145, 146, 147, 148, 149, 150], the small differences originating from the slightly different inputs adopted.

The A2HDM is not the most general version of a 2HDM without tree-level FC-

NCs. To avoid the unwanted FCNCs one just needs diagonal Yukawa matrices Y_f in the fermion mass-eigenstate basis, i.e. $Y_d = \mathrm{diag}(y_d, y_s, y_b)$, $Y_u = \mathrm{diag}(y_u, y_c, y_t)$ and $Y_l = \mathrm{diag}(y_e, y_\mu, y_\tau)$, with arbitrary parameters y_i. This more general scenario can be formally described by the Lagrangian (2.10) with the substitution $\varsigma_f M_f \to Y_f$. One could still use nine dimensionless parameters $\varsigma_f \equiv y_f/m_f$, one for each charged fermion [151], but in this case this is just a redefinition of the Yukawa couplings y_f because a priori nothing relates them to the fermion masses [152]. The hierarchy of couplings characteristic of the A2HDM ansatz is lost and one can no longer justify that the leading charged-scalar effects originate in the heavier fermion couplings (it becomes an assumption). With this caveat in mind, our results can still be applied in this case, but most correlations among different processes disappear because the associated constraints correspond now to different ς_f parameters. For instance, the constraint in (4.4) refers to $\sqrt{|\varsigma_\tau \varsigma_\mu^*|}$ and figures 1 to $\varsigma_\tau^* \varsigma_b$ (left) and $\varsigma_\mu^* \varsigma_c$ (right).

The A2HDM provides a general setting to discuss the phenomenology of 2HDMs, satisfying in a natural way the requirement of very suppressed FCNC effects. The alignment conditions imply Yukawa couplings proportional to the corresponding fermion masses, which is supported by the data (bounds of order 1 for the ς_f parameters). While including as limiting cases all $\mathcal{Z}_2$ models, the A2HDM incorporates possible new sources of CP violation through the ς_f phases. The additional freedom introduced by these phases makes easier to avoid some low-energy constraints, resulting in weaker limits than in the usual scenarios with discrete $\mathcal{Z}_2$ symmetries. A detailed analysis of CP-violating observables is clearly needed to investigate the allowed ranges for these phases and their potential phenomenological relevance [35].

At the moment, the data does not show any clear deviation from the SM. Therefore, we have derived upper limits on the Yukawa parameters. Nevertheless, we have already pointed out that the A2HDM could account for a sizeable B_s^0 mixing phase, as suggested by the present $B_s \to J/\psi\phi$ and like-sign dimuon data. Our bounds could be made stronger, adopting more aggressive estimates for the hadronic parameters entering the analysis, but we have preferred to be on the conservative side and infer solid limits for later use. Improvements are to be expected on one hand from better theoretical determinations of the hadronic inputs, and on the other hand from more accurate measurements at NA62 (kaons), LHCb ($\Delta m_{d,s}, B_s \to J/\psi\phi$), a future Super-B factory (τ, $b \to s\gamma, \Delta m_d, B \to \ell\nu, B \to D\ell\nu$), or a linear collider with Giga-Z option (R_b). The agreement of the different bounds in the vicinity of zero is trivial, when the SM agrees with the data. If signals for new-physics are found at LHC, the analysis presented here will be capable of quantifying the agreement (or disagreement) of the data with the A2HDM, and with the different implementations of the 2HDM based on $\mathcal{Z}_2$ symmetries, in one step.

Note added

After this work was finished, two relevant papers have been posted in the archives. In Ref. [153] an approximate solution to the renormalization-group equations of the A2HDM is analyzed and the generated FCNC terms are studied numerically; the results presented

there agree with our FCNC operator (2.13) and it is concluded that the induced FCNC effects are well below the present experimental bounds. Ref. [154] analyzes the strength of FCNC effects mediated by neutral scalars in a minimal-flavour-violating framework containing two Higgs doublets, assuming a perturbative expansion around the type II model. The tree-level alignment conditions of Ref. [1] are reproduced, the one-loop FCNC structures in (2.13) are discussed and their coefficients are estimated at large $\tan\beta$ in the decoupling limit. The phenomenological analysis of Ref. [154] emphasizes the potential relevance of the flavour-blind phases present in the A2HDM to accommodate the recent hints of a large B_s^0 mixing phase through neutral-Higgs exchange.

Acknowledgments

The authors would like to thank Mikolaj Misiak and Nazila Mahmoudi for helpful discussions, and Guiseppe Degrassi for clarifying comments on Eqs. (5.1) and (5.2). This work has been supported in part by the EU MRTN network FLAVIAnet [Contract No. MRTN-CT-2006-035482], by MICINN, Spain [Grants FPA2007-60323 and Consolider-Ingenio 2010 Program CSD2007-00042 –CPAN–] and by Generalitat Valenciana [Prometeo/2008/069]. The work of P.T. is funded through an FPU Grant (MICINN, Spain).

A. $\Delta F = 2$ effective Hamiltonian

A.1 $\Delta B = 2$

At lowest order, the $\Delta F = 2$ transitions are mediated by box diagrams with exchanges of $W^\pm$ and/or $H^\pm$ propagators. Performing the matching between the A2HDM amplitude and the low-energy effective Hamiltonian $\mathcal{H}_{\rm eff}^{\Delta F=2}$, at the scale $\mu_{tW} \sim M_W, m_t$, one obtains the Wilson coefficients $C_i(\mu)$. We have derived the LO results given in table 4, where $x_W \equiv m_t^2/M_W^2$ and $x_H \equiv m_t^2/M_{H^\pm}^2$. They can be expressed in terms of the two four-point functions [155]:

$$\begin{aligned} D_0(m_1,m_2,M_1,M_2) \equiv & \frac{m_2^2\,\log\left(\frac{m_2^2}{m_1^2}\right)}{(m_2^2-m_1^2)(m_2^2-M_1^2)(m_2^2-M_2^2)} + \\ & + \frac{M_1^2\,\log\left(\frac{M_1^2}{m_1^2}\right)}{(M_1^2-m_1^2)(M_1^2-m_2^2)(M_1^2-M_2^2)} + \\ & + \frac{M_2^2\,\log\left(\frac{M_2^2}{m_1^2}\right)}{(M_2^2-m_1^2)(M_2^2-m_2^2)(M_2^2-M_1^2)}\,, \end{aligned} \tag{A.1}$$

$$D_2(m_1,m_2,M_1,M_2) \equiv \frac{m_2^4\,\log\left(\frac{m_2^2}{m_1^2}\right)}{(m_2^2-m_1^2)(m_2^2-M_1^2)(m_2^2-M_2^2)} + \\ + \frac{M_1^4\,\log\left(\frac{M_1^2}{m_1^2}\right)}{(M_1^2-m_1^2)(M_1^2-m_2^2)(M_1^2-M_2^2)} + \\ + \frac{M_2^4\,\log\left(\frac{M_2^2}{m_1^2}\right)}{(M_2^2-m_1^2)(M_2^2-m_2^2)(M_2^2-M_1^2)}\,, \tag{A.2}$$

through $(i=0,2)$

$$D_i(m,M_1,M_2) \equiv \lim_{m_2\to m} D_i(m,m_2,M_1,M_2)\,, \tag{A.3}$$

$$D_i(m,M) \equiv \lim_{M_2\to M} D_i(m,M,M_2)\,, \tag{A.4}$$

$$\overline{D}_2(m,M_1,M_2) \equiv D_2(m,M_1,M_2) - D_2(0,M_1,M_2)\,. \tag{A.5}$$

These one-loop contributions involve virtual propagators of up-type quarks (u,c,t). Once the GIM cancellation is taken into account, the up and charm contributions vanish in the limit $m_{u,c}\to 0$, which we have adopted. Thus, the B meson mixing is completely dominated by the top-quark contributions (the different CKM factors have all a similar size for B_d^0 mixing, $V_{ud}^*V_{ub}\sim V_{cd}^*V_{cb}\sim V_{td}^*V_{tb}\sim A\lambda^3$, while in the B_s^0 case $V_{us}^*V_{ub}\sim A\lambda^4$ and $V_{cs}^*V_{cb}\sim V_{ts}^*V_{tb}\sim A\lambda^2$). Since the scalar couplings are proportional to quark masses, we have maintained the masses of the external down-type quarks. In the limit $m_d\to 0$, we reproduce the results given in [121]. The only Wilson coefficients which are not suppressed by powers of m_d are $C_{\rm VLL}$ and $C^1_{\rm SRR}$. Therefore, for all practical purposes, one can neglect the remaining operators.

The running for $\mathcal{O}_1^{SRR}$ is performed using the results of [119],

$$\begin{pmatrix} C^1_{\rm SRR}(\mu_b) \\ C^2_{\rm SRR}(\mu_b)\end{pmatrix} = \begin{pmatrix} [\eta_{11}(\mu_b)]_{\rm SRR} & [\eta_{12}(\mu_b)]_{\rm SRR} \\ [\eta_{21}(\mu_b)]_{\rm SRR} & [\eta_{22}(\mu_b)]_{\rm SRR}\end{pmatrix}\begin{pmatrix} C^1_{\rm SRR}(\mu_{tW}) \\ C^2_{\rm SRR}(\mu_{tW})\end{pmatrix}\,, \tag{A.6}$$

with

$$[\eta_{11}(\mu_b)]_{\rm SRR} = 1.0153\,\eta_5^{-0.6315} - 0.0153\,\eta_5^{0.7184}\,, \tag{A.7}$$

$$[\eta_{12}(\mu_b)]_{\rm SRR} = 1.9325\,(\eta_5^{-0.6315} - \eta_5^{0.7184})\,, \tag{A.8}$$

$$[\eta_{21}(\mu_b)]_{\rm SRR} = 0.0081\,(\eta_5^{0.7184} - \eta_5^{-0.6315})\,, \tag{A.9}$$

$$[\eta_{22}(\mu_b)]_{\rm SRR} = 1.0153\,\eta_5^{0.7184} - 0.0153\,\eta_5^{-0.6315}\,. \tag{A.10}$$

These are leading-order expressions, but they have been evaluated with the two-loop expression for α_s in $\eta_5=\frac{\alpha_s^{(5)}(\mu_{tW})}{\alpha_s^{(5)}(\mu_b)}\sim 0.7$.

The corresponding matrix elements are given by

$$\langle\mathcal{O}^{\rm VLL}\rangle(\mu) = \frac{1}{3}m_{B_d^0}f^2_{B_d^0}B^{\rm VLL}(\mu)\,, \tag{A.11}$$

$$\langle\mathcal{O}_1^{\rm SRR}\rangle(\mu) = -\frac{5}{24}\left(\frac{m_{B_d^0}}{m_b(\mu)+m_d(\mu)}\right)^2 m_{B_d^0}f^2_{B_d^0}B_1^{\rm SRR}(\mu)\,, \tag{A.12}$$

$$\langle\mathcal{O}_2^{\rm SRR}\rangle(\mu) = -\frac{1}{2}\left(\frac{m_{B_d^0}}{m_b(\mu)+m_d(\mu)}\right)^2 m_{B_d^0}f^2_{B_d^0}B_2^{\rm SRR}(\mu)\,, \tag{A.13}$$

$\mathcal{O}_i$	$C_i(\mu_{tW})$
$\mathcal{O}^{\rm VLL}$	$(4x_W + x_W^2)M_W^2 D_2(m_t, M_W) - 8x_W^2 M_W^4 D_0(m_t, M_W) +$ $+ 2\lvert\varsigma_u\rvert^2 x_W^2 \left[M_W^2 D_2(m_t, M_W, M_{H^\pm}) - 4M_W^4 D_0(m_t, M_W, M_{H^\pm})\right] +$ $+ \lvert\varsigma_u\rvert^4 x_W^2 M_W^2 D_2(m_t, M_{H^\pm})$
$\mathcal{O}^{\rm VRR}$	$\frac{m_d^2 m_b^2}{M_W^4}\left[\lvert\varsigma_d\rvert^4 x_H M_W^2 D_2(m_t, M_{H^\pm}) + \lvert\varsigma_d\rvert^2 M_W^2 \overline{D}_2(m_t, M_W, M_{H^\pm})\right]$
$\mathcal{O}_1^{\rm LR}$	$2\frac{m_d m_b}{M_W^2} x_W \left[\lvert\varsigma_d\rvert^2\lvert\varsigma_u\rvert^2 M_W^2 D_2(m_t, M_{H^\pm}) + 2\,{\rm Re}(\varsigma_d^*\varsigma_u) M_W^2 D_2(m_t, M_W, M_{H^\pm})\right]$
$\mathcal{O}_2^{\rm LR}$	$2\frac{m_d m_b}{M_W^2}\left[4\lvert\varsigma_d\rvert^2\lvert\varsigma_u\rvert^2 x_W M_W^4 D_0(m_t, M_{H^\pm}) - 4\lvert\varsigma_d\rvert^2 M_W^2 \overline{D}_2(m_t, M_W, M_{H^\pm}) +\right.$ $\left. + (\lvert\varsigma_d\rvert^2 + \lvert\varsigma_u\rvert^2) x_W M_W^2 D_2(m_t, M_W, M_{H^\pm})\right]$
$\mathcal{O}_1^{\rm SLL}$	$4\frac{m_d^2}{M_W^2} x_W^2 \left[(\varsigma_u\varsigma_d^*)^2 M_W^4 D_0(m_t, M_{H^\pm}) + 2\varsigma_u\varsigma_d^* M_W^4 D_0(m_t, M_W, M_{H^\pm})\right]$
$\mathcal{O}_2^{\rm SLL}$	0
$\mathcal{O}_1^{\rm SRR}$	$4\frac{m_b^2}{M_W^2} x_W^2 \left[(\varsigma_d\varsigma_u^*)^2 M_W^4 D_0(m_t, M_{H^\pm}) + 2\varsigma_d\varsigma_u^* M_W^4 D_0(m_t, M_W, M_{H^\pm})\right]$
$\mathcal{O}_2^{\rm SRR}$	0

Table 4: Leading-order Wilson coefficients for the $\Delta B = 2$ operators given above. The quark masses from the scalar couplings are to be taken at the matching scale μ_{tW}.

the $B_i(\mu)$ parametrizing the deviation from the naive factorization limit. These $B_i(\mu)$ factors have been evaluated in the quenched approximation on the lattice in [156], using a different operator basis. The connection reads (see again [119], given here with both operators in the same scheme)

$$B_1^{\rm SRR}(\mu) \;=\; B_2(\mu)\,, \qquad\qquad B_2^{\rm SRR}(\mu) \;=\; \frac{5}{3}B_2(\mu) - \frac{2}{3}B_3(\mu)\,. \tag{A.14}$$

From [156] we arrive at the values given in table 5 by adding again all systematic uncertainties linearly.

	B_d^0	B_s^0
$B_2^{\overline{MS}}(m_b)$	$0.83 \pm 0.03 \pm 0.06$	$0.84 \pm 0.02 \pm 0.06$
$B_3^{\overline{MS}}(m_b)$	$0.90 \pm 0.06 \pm 0.12$	$0.91 \pm 0.03 \pm 0.12$

Table 5: B-parameters for $B_{d,s}^0$ mixing from [156]. Systematic errors added linearly.

The wanted B_d^0-$\bar{B}_d^0$ mixing amplitude is given by

$$\begin{aligned}\langle B^0|\mathcal{H}_{\rm eff}^{\Delta B=2}|\bar{B}^0\rangle \;=\; & \frac{G_F^2 M_W^2}{16\pi^2}(V_{td}^* V_{tb})^2 f_{B_d^0}^2 M_{B_d^0}^2 \times \\ & \times \left[\frac{2}{3}\,\hat{B}_{B_d^0}\,\eta_B(x_W, x_H)\,C_{\rm VLL}(\mu_{tW}) + \right. \\ & \left. + \frac{m_{B_D^0}^2}{(m_b(\mu_b) + m_d(\mu_b))^2}\left[\eta_{\rm SRR}(\mu_b, \mu_{tW})\,\mathbf{C}_{\rm SRR}(\mu_{tW})\right]^T \mathbf{B}_{\rm SRR}(\mu_b)\right]\,,\end{aligned} \tag{A.15}$$

with

$$\mathbf{B}_{\rm SRR}(\mu_b) = \begin{pmatrix} -\frac{5}{12}B_{2,d}(\mu_b) \\ \frac{2}{3}B_{3,d}(\mu_b) - \frac{5}{3}B_{2,d}(\mu_b) \end{pmatrix} . \tag{A.16}$$

From this, we get the relevant observables as

$$\Delta m_{B_d^0} = \frac{1}{m_{B_d^0}} |\langle B_d^0 | \mathcal{H}_{\rm eff}^{\Delta B=2} | \bar{B}_d^0 \rangle| \,, \tag{A.17}$$

$$\phi_{B_d^0} = -{\rm Arg}\left[\langle B_d^0 | \mathcal{H}_{\rm eff}^{\Delta B=2} | \bar{B}_d^0 \rangle\right] . \tag{A.18}$$

The analogous expressions for B_s^0-$\bar{B}_s^0$ mixing are trivially obtained changing the label d to s everywhere.

A.2 $\Delta S = 2$

For the Kaon mixing amplitude, we have calculated the LO matching coefficients completely anologous to the $\Delta B = 2$ coefficients, keeping the charm mass finite. Due to the strong suppression of all other operators by light quark masses we can choose the LO matching coefficients to be

$$\begin{aligned}
C^{cc}_{\mathcal{O}_{\rm VLL}} &= (4x_W^{cc} + x_W^{cc\,2}) M_W^2 D_2(m_c, M_W) - 8 x_W^{cc\,2} M_W^4 D_0(m_c, M_W) \,, \\
C^{ct}_{\mathcal{O}_{\rm VLL}} &= (4x_W^{ct} + x_W^{ct\,2}) M_W^2 D_2(m_c, m_t, M_W) - 8 x_W^{ct\,2} M_W^4 D_0(m_c, m_t, M_W) + \\
&\quad + 2|\varsigma_u|^2 x_W^{ct\,2} \left[M_W^2 D_2(m_c, m_t, M_W, M_{H^\pm}) - 4 M_W^4 D_0(m_c, m_t, M_W, M_{H^\pm}) \right] + \\
&\quad + |\varsigma_u|^4 x_W^{ct\,2} M_W^2 D_2(m_c, m_t, M_{H^\pm}) \,, \\
C^{tt}_{\mathcal{O}_{\rm VLL}} &= (4x_W + x_W^2) M_W^2 D_2(m_t, M_W) - 8 x_W^2 M_W^4 D_0(m_t, M_W) + \\
&\quad + 2|\varsigma_u|^2 x_W^2 \left[M_W^2 D_2(m_t, M_W, M_{H^\pm}) - 4 M_W^4 D_0(m_t, M_W, M_{H^\pm}) \right] + \\
&\quad + |\varsigma_u|^4 x_W^2 M_W^2 D_2(m_t, M_{H^\pm}) \,, \\
C_{\mathcal{O}_i} &= 0 \quad (i \neq {\rm VLL}) \,,
\end{aligned} \tag{A.19}$$

where the loop functions $D_{0,2}$ have been defined in appendix A, and $x_W^{ct} = m_c m_t / M_W^2$. In the calculation, we use the NLO results for the SM which have been calculated in [157, 158], while the NLO charged scalar contributions to the top contribution are again taken from [121], corrected and applied to our scenario.

References

[1] A. Pich and P. Tuzon, *Yukawa Alignment in the Two-Higgs-Doublet Model*, *Phys. Rev.* **D80** (2009) 091702, [arXiv:0908.1554 [hep-ph]].

[2] J. Gunion, H. Haber, G. Kane, and S. Dawson, *The Higgs Hunters Guide*. Addison-Wesley, New York, 1990.

[3] G. C. Branco, L. Lavoura, and J. P. Silva, *CP Violation*. Oxford University Press, Oxford, England, 1999.

[4] S. L. Glashow and S. Weinberg, *Natural Conservation Laws for Neutral Currents*, *Phys. Rev.* **D15** (1977) 1958.

[5] H. E. Haber, G. L. Kane, and T. Sterling, *The Fermion Mass Scale and Possible Effects of Higgs Bosons on Experimental Observables*, *Nucl. Phys.* **B161** (1979) 493.

[6] L. J. Hall and M. B. Wise, *Flavor changing higgs-boson couplings*, *Nucl. Phys.* **B187** (1981) 397.

[7] J. F. Donoghue and L. F. Li, *Properties of Charged Higgs Bosons*, *Phys. Rev.* **D19** (1979) 945.

[8] V. D. Barger, J. L. Hewett, and R. J. N. Phillips, *New constraints on the charged higgs sector in two higgs doublet models*, *Phys. Rev.* **D41** (1990) 3421.

[9] M. J. Savage, *Constraining flavor changing neutral currents with $B \to \mu^+\mu^-$*, *Phys. Lett.* **B266** (1991) 135–141.

[10] Y. Grossman, *Phenomenology of models with more than two Higgs doublets*, *Nucl. Phys.* **B426** (1994) 355–384, [arXiv:hep-ph/9401311].

[11] A. G. Akeroyd, *Fermiophobic and other non-minimal neutral Higgs bosons at the LHC*, *J. Phys.* **G24** (1998) 1983–1994, [arXiv:hep-ph/9803324].

[12] A. G. Akeroyd, *Non-minimal neutral Higgs bosons at LEP2*, *Phys. Lett.* **B377** (1996) 95–101, [arXiv:hep-ph/9603445].

[13] A. G. Akeroyd and W. J. Stirling, *Light charged Higgs scalars at high-energy e^+e^- colliders*, *Nucl. Phys.* **B447** (1995) 3–17.

[14] M. Aoki, S. Kanemura, K. Tsumura, and K. Yagyu, *Models of Yukawa interaction in the two Higgs doublet model, and their collider phenomenology*, *Phys. Rev.* **D80** (2009) 015017, [arXiv:0902.4665 [hep-ph]].

[15] E. Ma, *Utility of a Special Second Scalar Doublet*, *Mod. Phys. Lett.* **A23** (2008) 647–652, [arXiv:0802.2917 [hep-ph]].

[16] E. Ma, *Verifiable radiative seesaw mechanism of neutrino mass and dark matter*, *Phys. Rev.* **D73** (2006) 077301, [arXiv:hep-ph/0601225].

[17] R. Barbieri, L. J. Hall, and V. S. Rychkov, *Improved naturalness with a heavy Higgs: An alternative road to LHC physics*, *Phys. Rev.* **D74** (2006) 015007, [arXiv:hep-ph/0603188].

[18] L. Lopez Honorez, E. Nezri, J. F. Oliver, and M. H. G. Tytgat, *The inert doublet model: An archetype for dark matter*, *JCAP* **0702** (2007) 028, [arXiv:hep-ph/0612275].

[19] N. Cabibbo, *Unitary Symmetry and Leptonic Decays*, *Phys. Rev. Lett.* **10** (1963) 531–533.

[20] M. Kobayashi and T. Maskawa, *CP Violation in the Renormalizable Theory of Weak Interaction*, *Prog. Theor. Phys.* **49** (1973) 652–657.

[21] T. P. Cheng and M. Sher, *Mass Matrix Ansatz and Flavor Nonconservation in Models with Multiple Higgs Doublets*, *Phys. Rev.* **D35** (1987) 3484.

[22] D. Atwood, L. Reina, and A. Soni, *Phenomenology of two Higgs doublet models with flavor changing neutral currents*, *Phys. Rev.* **D55** (1997) 3156–3176, [arXiv:hep-ph/9609279].

[23] J. L. Diaz-Cruz, R. Noriega-Papaqui, and A. Rosado, *Measuring the fermionic couplings of the Higgs boson at future colliders as a probe of a non-minimal flavor structure*, *Phys. Rev.* **D71** (2005) 015014, [arXiv:hep-ph/0410391].

[24] J. L. Diaz-Cruz, J. Hernandez-Sanchez, S. Moretti, R. Noriega-Papaqui, and A. Rosado, *Yukawa Textures and Charged Higgs Boson Phenomenology in the 2HDM-III*, *Phys. Rev.* **D79** (2009) 095025, [arXiv:0902.4490 [hep-ph]].

[25] S. Davidson and H. E. Haber, *Basis-independent methods for the two-Higgs-doublet model*, *Phys. Rev.* **D72** (2005) 035004, [arXiv:hep-ph/0504050].

[26] P. M. Ferreira, L. Lavoura, and J. P. Silva, *Renormalization-group constraints on Yukawa alignment in multi-Higgs-doublet models*, *Phys. Lett.* **B688** (2010) 341–344, [arXiv:1001.2561 [hep-ph]].

[27] G. D'Ambrosio, G. F. Giudice, G. Isidori, and A. Strumia, *Minimal flavour violation: An effective field theory approach*, *Nucl. Phys.* **B645** (2002) 155–187, [arXiv:hep-ph/0207036].

[28] R. S. Chivukula and H. Georgi, *Composite Technicolor Standard Model*, *Phys. Lett.* **B188** (1987) 99.

[29] L. J. Hall and L. Randall, *Weak scale effective supersymmetry*, *Phys. Rev. Lett.* **65** (1990) 2939–2942.

[30] A. J. Buras, P. Gambino, M. Gorbahn, S. Jager, and L. Silvestrini, *Universal unitarity triangle and physics beyond the standard model*, *Phys. Lett.* **B500** (2001) 161–167, [arXiv:hep-ph/0007085].

[31] V. Cirigliano, B. Grinstein, G. Isidori, and M. B. Wise, *Minimal flavor violation in the lepton sector*, *Nucl. Phys.* **B728** (2005) 121–134, [arXiv:hep-ph/0507001].

[32] A. L. Kagan, G. Perez, T. Volansky, and J. Zupan, *General Minimal Flavor Violation*, *Phys. Rev.* **D80** (2009) 076002, [arXiv:0903.1794 [hep-ph]].

[33] F. J. Botella, G. C. Branco, and M. N. Rebelo, *Minimal Flavour Violation and Multi-Higgs Models*, *Phys. Lett.* **B687** (2010) 194–200, [arXiv:0911.1753 [hep-ph]].

[34] G. Cvetic, C. S. Kim, and S. S. Hwang, *Higgs-mediated flavor-changing neutral currents in the general framework with two Higgs doublets: An RGE analysis*, *Phys. Rev.* **D58** (1998) 116003, [arXiv:hep-ph/9806282].

[35] M. Jung, A. Pich, and P. Tuzón, *Work in progress*, .

[36] **D0** Collaboration, V. M. Abazov *et al.*, *Evidence for an anomalous like-sign dimuon charge asymmetry*, *arXiv:1005.2757 [hep-ex]* (2010).

[37] B. A. Dobrescu, P. J. Fox, and A. Martin, *CP violation in B_s mixing from heavy Higgs exchange*, *arXiv:*1005.4238 [hep-ph] (2010).

[38] A. Wahab El Kaffas, P. Osland, and O. M. Ogreid, *Constraining the Two-Higgs-Doublet-Model parameter space*, *Phys. Rev.* **D76** (2007) 095001, [arXiv:0706.2997 [hep-ph]].

[39] O. Deschamps *et al.*, *The Two Higgs Doublet of Type II facing flavour physics data*, *arXiv:*0907.5135 [hep-ph] (2009).

[40] H. Flacher *et al.*, *Gfitter - Revisiting the Global Electroweak Fit of the Standard Model and Beyond*, *Eur. Phys. J.* **C60** (2009) 543–583, [arXiv:0811.0009 [hep-ph]].

[41] **UTfit** Collaboration, M. Bona *et al.*, *An Improved Standard Model Prediction Of $BR(B \to \tau\nu)$ And Its Implications For New Physics*, *Phys. Lett.* **B687** (2010) 61–69, [arXiv:0908.3470 [hep-ph]].

[42] F. Mahmoudi and O. Stal, *Flavor constraints on the two-Higgs-doublet model with general Yukawa couplings*, *Phys. Rev.* **D81** (2010) 035016, [arXiv:0907.1791 [hep-ph]].

[43] A. Hocker, H. Lacker, S. Laplace, and F. Le Diberder, *A New approach to a global fit of the CKM matrix*, *Eur. Phys. J.* **C21** (2001) 225–259, [arXiv:hep-ph/0104062].

[44] **CKMfitter Group**, *Average of lattice QCD inputs for CKM fits*, http://ckmfitter.in2p3.fr/plots_Beauty09/latticeinputs280809.pdf (2009).

[45] G. Colangelo, *The FLAG working group: status report*, in *EuroFlavour09 - Bari*, 2009.

[46] V. Lubicz, *Kaon physics from lattice QCD*, *PoS* **LAT2009** (2009) 013, [arXiv:1004.3473 [hep-lat]].

[47] P. A. Boyle *et al.*, *$K \to \pi$ form factors with reduced model dependence*, *arXiv:1004.0886 [hep-lat]* (2010).

[48] P. A. Boyle *et al.*, *K_{l3} semileptonic form factor from 2+1 flavour lattice QCD*, *Phys. Rev. Lett.* **100** (2008) 141601, [arXiv:0710.5136 [hep-lat]].

[49] V. Lubicz, F. Mescia, S. Simula, C. Tarantino, and f. t. E. Collaboration, *$K \to \pi l \nu$ Semileptonic Form Factors from Two-Flavor Lattice QCD*, *Phys. Rev.* **D80** (2009) 111502, [arXiv:0906.4728 [hep-lat]].

[50] H. Leutwyler and M. Roos, *Determination of the Elements V_{us} and V_{ud} of the Kobayashi-Maskawa Matrix*, *Z. Phys.* **C25** (1984) 91.

[51] J. Bijnens and P. Talavera, *K_{l3} decays in chiral perturbation theory*, *Nucl. Phys.* **B669** (2003) 341–362, [arXiv:hep-ph/0303103].

[52] M. Jamin, J. A. Oller, and A. Pich, *Order p^6 chiral couplings from the scalar $K\pi$ form-factor*, *JHEP* **02** (2004) 047, [arXiv:hep-ph/0401080].

[53] V. Cirigliano *et al.*, *The $\langle SPP \rangle$ Green function and SU(3) breaking in K_{l3} decays*, *JHEP* **04** (2005) 006, [arXiv:hep-ph/0503108].

[54] A. Kastner and H. Neufeld, *The K_{l3} scalar form factors in the standard model*, *Eur. Phys. J.* **C57** (2008) 541–556, [arXiv:0805.2222 [hep-ph]].

[55] M. Wingate, C. T. H. Davies, A. Gray, G. P. Lepage, and J. Shigemitsu, *The B_s and D_s decay constants in 3 flavor lattice QCD*, *Phys. Rev. Lett.* **92** (2004) 162001, [arXiv:hep-ph/0311130].

[56] **HPQCD** Collaboration, E. Gamiz, C. T. H. Davies, G. P. Lepage, J. Shigemitsu, and M. Wingate, *Neutral B Meson Mixing in Unquenched Lattice QCD*, *Phys. Rev.* **D80** (2009) 014503, [arXiv:0902.1815 [hep-lat]].

[57] C. Bernard *et al.*, *B and D Meson Decay Constants*, *PoS* **LATTICE2008** (2008) 278, [arXiv:0904.1895 [hep-lat]].

[58] **HPQCD** Collaboration, E. Follana, C. T. H. Davies, G. P. Lepage, and J. Shigemitsu, *High Precision determination of the π, K, D and D_s decay constants from lattice QCD*, *Phys. Rev. Lett.* **100** (2008) 062002, [arXiv:0706.1726 [hep-lat]].

[59] C. Bernard *et al.*, *Status of the MILC light pseudoscalar meson project*, *PoS* **LAT2007** (2007) 090, [arXiv:0710.1118 [hep-lat]].

[60] S. Durr *et al.*, *The ratio F_K/F_π in QCD*, *Phys. Rev.* **D81** (2010) 054507, [arXiv:1001.4692 [hep-lat]].

[61] C. Aubin, J. Laiho, and R. S. Van de Water, *The neutral kaon mixing parameter B_K from unquenched mixed-action lattice QCD*, *Phys. Rev.* **D81** (2010) 014507, [arXiv:0905.3947 [hep-lat]].

[62] **RBC** Collaboration, C. Kelly, P. A. Boyle, and C. T. Sachrajda, *Continuum results for light hadrons from 2+1 flavor DWF ensembles*, *PoS* **LAT2009** (2009) 087, [arXiv:0911.1309 [hep-lat]].

[63] J. C. Hardy and I. S. Towner, *Superallowed 0^+ to 0^+ nuclear beta decays: A new survey with precision tests of the conserved vector current hypothesis and the standard model*, *Phys. Rev.* **C79** (2009) 055502, [arXiv:0812.1202 [nucl-ex]].

[64] M. Antonelli *et al.*, *Flavor Physics in the Quark Sector*, *arXiv:*0907.5386 [hep-ph] (2009).

[65] **HFAG**, E. Barberio *et al.*, *Averages of b−hadron and c−hadron Properties at the End of 2007*, *arXiv:*0808.1297 [hep-ex] (2008). Online update available at http://www.slac.stanford.edu/xorg/hfag.

[66] **Particle Data Group**, C. Amsler *et al.*, *Review of particle physics*, *Phys. Lett.* **B667** (2008) 1. Online updates: http://pdg.lbl.gov.

[67] Tevatron Electroweak Working Group, *Combination of CDF and D0 Results on the Mass of the Top Quark*, *arXiv:*0903.2503 [hep-ex] (2009).

[68] W. J. Marciano, *Precise determination of $|V_{us}|$ from lattice calculations of pseudoscalar decay constants*, *Phys. Rev. Lett.* **93** (2004) 231803, [arXiv:hep-ph/0402299].

[69] V. Cirigliano and I. Rosell, *$\pi/K \to e\nu$ branching ratios to $O(e^2p^4)$ in Chiral Perturbation Theory*, *JHEP* **10** (2007) 005, [arXiv:0707.4464 [hep-ph]].

[70] V. Cirigliano and I. Rosell, *Two-loop effective theory analysis of $\pi(K) \to e\bar{\nu}_e(\gamma)$ branching ratios*, *Phys. Rev. Lett.* **99** (2007) 231801, [arXiv:0707.3439 [hep-ph]].

[71] M. Antonelli *et al.*, *An evaluation of $|V_{us}|$ and precise tests of the Standard Model from world data on leptonic and semileptonic kaon decays*, *arXiv:*1005.2323 [hep-ph] (2010).

[72] R. Decker and M. Finkemeier, *Short and long distance effects in the decay $\tau \to \pi\nu_\tau(\gamma)$*, *Nucl. Phys.* **B438** (1995) 17–53, [arXiv:hep-ph/9403385].

[73] R. Decker and M. Finkemeier, *Radiative corrections to the decay $\tau \to \pi\nu_\tau$*, *Nucl. Phys. Proc. Suppl.* **40** (1995) 453–461, [arXiv:hep-ph/9411316].

[74] W. J. Marciano and A. Sirlin, *Radiative corrections to $\pi_{\ell 2}$ decays*, *Phys. Rev. Lett.* **71** (1993) 3629–3632.

[75] G. M. de Divitiis, R. Petronzio, and N. Tantalo, *Quenched lattice calculation of semileptonic heavy-light meson form factors*, *JHEP* **10** (2007) 062, [arXiv:0707.0587 [hep-lat]].

[76] The ALEPH, DELPHI, L3 and OPAL collaborations, *Precision electroweak measurements on the Z resonance*, *Phys. Rept.* **427** (2006) 257, [arXiv:hep-ex/0509008].

[77] G. Degrassi and P. Slavich, *QCD Corrections in two-Higgs-doublet extensions of the Standard Model with Minimal Flavor Violation*, *Phys. Rev.* **D81** (2010) 075001, [arXiv:1002.1071 [hep-ph]].

[78] A. J. Buras, D. Guadagnoli, and G. Isidori, *On ϵ_K beyond lowest order in the Operator Product Expansion*, *Phys. Lett.* **B688** (2010) 309–313, [arXiv:1002.3612 [hep-ph]].

[79] **UTfit** Collaboration, M. Bona *et al.*, *The 2004 UTfit Collaboration report on the status of the unitarity triangle in the standard model*, *JHEP* **07** (2005) 028, [arXiv:hep-ph/0501199]. For updated results and plots see: http://utfit.org.

[80] **CKMfitter Group**, J. Charles *et al.*, *CP violation and the CKM matrix: Assessing the impact of the asymmetric B factories*, *Eur. Phys. J.* **C41** (2005) 1–131, [arXiv:hep-ph/0406184]. Updated results and plots available at: http://ckmfitter.in2p3.fr.

[81] The LEP Working Group for Higgs boson searches, *Search for charged Higgs bosons: Preliminary combined results using LEP data collected at energies up to 209 GeV*, *arXiv:*hep-ex/0107031 (2001).

[82] **OPAL** Collaboration, G. Abbiendi *et al.*, *Search for Charged Higgs Bosons in e^+e^- Collisions at $\sqrt{s}$=189-209 GeV*, *arXiv:*0812.0267 [hep-ex] (2008).

[83] **BABAR** Collaboration, B. Aubert *et al.*, *Measurements of Charged Current Lepton Universality and $|V_{us}|$ using Tau Lepton Decays to $e^-\bar{\nu}_e\nu_\tau$, $\mu^-\bar{\nu}_\mu\nu_\tau$, $\pi^-\nu_\tau$ and $K^-\nu_\tau$*, *arXiv:*0912.0242 [hep-ex] (2009).

[84] **CLEO** Collaboration, B. I. Eisenstein *et al.*, *Precision Measurement of $B(D^+ \to \mu^+\nu)$ and the Pseudoscalar Decay Constant f_{D^+}*, *Phys. Rev.* **D78** (2008) 052003, [arXiv:0806.2112 [hep-ex]].

[85] **CLEO** Collaboration, J. P. Alexander *et al.*, *Measurement of $BR(D_s^+ \to \ell^+\nu)$ and the Decay Constant $f_{D_s^+}$ From 600 /pb^{-1} of $e^\pm$ Annihilation Data Near 4170 MeV*, *Phys. Rev.* **D79** (2009) 052001, [arXiv:0901.1216 [hep-ex]].

[86] **CLEO** Collaboration, P. U. E. Onyisi *et al.*, *Improved Measurement of Absolute Branching Fraction of $D_s \to \tau\nu$*, *Phys. Rev.* **D79** (2009) 052002, [arXiv:0901.1147 [hep-ex]].

[87] **CLEO** Collaboration, P. Naik *et al.*, *Measurement of the Pseudoscalar Decay Constant f_{D_s} Using $D_s^+ \to \tau^+\nu$, $\tau^+ \to \rho^+\bar{\nu}$ Decays*, *Phys. Rev.* **D80** (2009) 112004, [arXiv:0910.3602 [hep-ex]].

[88] **BABAR** Collaboration, J. P. Lees *et al.*, *Measurement of the Branching Fraction for $D_s^+ \to \tau^+\nu_\tau$ and Extraction of the Decay Constant f_{D_s}*, *arXiv:1003.3063 [hep-ex]* (2010).

[89] J. L. Rosner and S. Stone, *Leptonic Decays of Charged Pseudoscalar Mesons*, *arXiv:*1002.1655 [hep-ex] (2010). Prepared for the PDG report 2010.

[90] **Belle** Collaboration, L. Widhalm et al., *Measurement of $B(D_s \to \mu\nu)$)*, *Phys. Rev. Lett.* **100** (2008) 241801, [arXiv:0709.1340 [hep-ex]].

[91] **KLOE** Collaboration, F. Ambrosino *et al.*, *Measurement of the $K_L \to \pi\mu\nu$ form factor parameters with the KLOE detector*, *JHEP* **12** (2007) 105, [arXiv:0710.4470 [hep-ex]].

[92] **KTeV** Collaboration, E. Abouzaid *et al.*, *Dispersive analysis of $K_{L\mu3}$ and K_{Le3} scalar and vector form factors using KTeV data*, *Phys. Rev.* **D81** (2010) 052001, [arXiv:0912.1291 [hep-ex]].

[93] **BABAR** Collaboration, B. Aubert *et al.*, *Measurement of the Semileptonic Decays $B \to D\tau^-\bar{\nu}_\tau$ and $B \to D^*\tau^-\bar{\nu}_\tau$*, *Phys. Rev.* **D79** (2009) 092002, [arXiv:0902.2660 [hep-ex]].

[94] **Belle** Collaboration, A. Bozek and M. R. e. al., *Observation of $B^+ \to \bar{D}^{*0}\tau^+\nu_\tau$ and Evidence for $B^+ \to \bar{D}^0\tau^+\nu_\tau$ at Belle*, *arXiv:*1005.2302 [hep-ex] (2010).

[95] **Belle** Collaboration, I. Adachi *et al.*, *Measurement of $B \to D^{(*)}\tau\nu$ using full reconstruction tags*, *arXiv:*0910.4301 [hep-ex] (2009).

[96] ALEPH, CDF, D0, DELPHI, L3, OPAL and SLD Collaborations, *Precision Electroweak Measurements and Constraints on the Standard Model*, *arXiv:*0911.2604 [hep-ex] (2009).

[97] A. Pich, *Tau Physics: Theory Overview*, *Nucl. Phys. Proc. Suppl.* **181-182** (2008) 300–305, [arXiv:0806.2793 [hep-ph]].

[98] A. Pich, *Tau physics*, *Adv. Ser. Direct. High Energy Phys.* **15** (World Scientific, Singapore, 1998) 453–492, [arXiv:hep-ph/9704453].

[99] A. Pich and J. P. Silva, *Constraining new interactions with leptonic τ decays*, *Phys. Rev.* **D52** (1995) 4006–4018, [arXiv:hep-ph/9505327].

[100] W. J. Marciano and A. Sirlin, *Electroweak Radiative Corrections to tau Decay*, *Phys. Rev. Lett.* **61** (1988) 1815–1818.

[101] A. J. Buras, P. H. Chankowski, J. Rosiek, and L. Slawianowska, *$\Delta M_{d,s}$, $B^0_{d,s} \to \mu^+\mu^-$ and $B \to X_s\gamma$ in supersymmetry at large* $\tan\beta$, *Nucl. Phys.* **B659** (2003) 3, [arXiv:hep-ph/0210145].

[102] A. G. Akeroyd and S. Recksiegel, *The effect of $H^\pm$ on $B^\pm \to \tau^\pm\nu_\tau$ and $B^\pm \to \mu^\pm\nu_\mu$*, *J. Phys.* **G29** (2003) 2311–2317, [arXiv:hep-ph/0306037].

[103] G. Burdman, J. T. Goldman, and D. Wyler, *Radiative Leptonic Decays of Heavy Mesons*, *Phys. Rev.* **D51** (1995) 111–117, [arXiv:hep-ph/9405425].

[104] J. F. Kamenik and F. Mescia, *$B \to D\tau\nu$ Branching Ratios: Opportunity for Lattice QCD and Hadron Colliders*, *Phys. Rev.* **D78** (2008) 014003, [arXiv:0802.3790 [hep-ph]].

[105] U. Nierste, S. Trine, and S. Westhoff, *Charged-Higgs effects in a new $B \to D\tau\nu$ differential decay distribution*, *Phys. Rev.* **D78** (2008) 015006, [arXiv:0801.4938 [hep-ph]].

[106] C. G. Callan and S. B. Treiman, *Equal Time Commutators and K Meson Decays*, *Phys. Rev. Lett.* **16** (1966) 153–157.

[107] R. F. Dashen and M. Weinstein, *Theorem on the form-factors in K_{l3} decay*, *Phys. Rev. Lett.* **22** (1969) 1337–1340.

[108] J. Gasser and H. Leutwyler, *Low-Energy Expansion of Meson Form-Factors*, *Nucl. Phys.* **B250** (1985) 517–538.

[109] E. Passemar, *Precision SM calculations and theoretical interests beyond the SM in K_{l2} and K_{l3} decays*, *PoS* **KAON09** (2009) 024, [arXiv:1003.4696 [hep-ph]].

[110] V. Bernard, M. Oertel, E. Passemar, and J. Stern, *$K_L^{\mu 3}$ decay: A stringent test of right-handed quark currents*, *Phys. Lett.* **B638** (2006) 480, [arXiv:hep-ph/0603202].

[111] **NA48** Collaboration, A. Lai *et al.*, *Measurement of* $\mathrm{K}^0_{\mu 3}$ *form factors*, *Phys. Lett.* **B647** (2007) 341–350, [arXiv:hep-ex/0703002].

[112] J. Bernabeu, A. Pich, and A. Santamaria, *$\Gamma(Z \to b\bar{b})$: A Signature of Hard Mass Terms for a Heavy Top*, *Phys. Lett.* **B200** (1988) 569.

[113] J. Bernabeu, A. Pich, and A. Santamaria, *Top quark mass from radiative corrections to the $Z \to b\bar{b}$ decay*, *Nucl. Phys.* **B363** (1991) 326–344.

[114] H. E. Haber and H. E. Logan, *Radiative corrections to the $Zb\bar{b}$ vertex and constraints on extended Higgs sectors*, *Phys. Rev.* **D62** (2000) 015011, [arXiv:hep-ph/9909335].

[115] J. H. Field, *Indications for an anomalous righthanded coupling of the b-quark from a model independent analysis of LEP and SLD data on Z decays*, *Mod. Phys. Lett.* **A13** (1998) 1937–1954, [arXiv:hep-ph/9801355].

[116] K. G. Chetyrkin, J. H. Kuhn, and A. Kwiatkowski, *QCD corrections to the e^+e^- cross-section and the Z boson decay rate: Concepts and results*, *Phys. Rept.* **277** (1996) 189–281.

[117] J. M. Gerard, W. Grimus, A. Raychaudhuri, and G. Zoupanos, *Super Kobayashi-Maskawa CP Violation*, *Phys. Lett.* **B140** (1984) 349.

[118] F. Gabbiani, E. Gabrielli, A. Masiero, and L. Silvestrini, *A complete analysis of FCNC and CP constraints in general SUSY extensions of the standard model*, *Nucl. Phys.* **B477** (1996) 321–352, [arXiv:hep-ph/9604387].

[119] A. J. Buras, S. Jager, and J. Urban, *Master formulae for $\Delta F = 2$ NLO-QCD factors in the standard model and beyond*, *Nucl. Phys.* **B605** (2001) 600–624, [arXiv:hep-ph/0102316].

[120] D. Becirevic *et al.*, *$B_d - \bar{B}_d$ mixing and the $B_d \to J/\psi K_s$ asymmetry in general SUSY models*, *Nucl. Phys.* **B634** (2002) 105–119, [arXiv:hep-ph/0112303].

[121] J. Urban, F. Krauss, U. Jentschura, and G. Soff, *Next-to-leading order QCD corrections for the B^0-$\bar{B}^0$ mixing with an extended Higgs sector*, *Nucl. Phys.* **B523** (1998) 40–58, [arXiv:hep-ph/9710245].

[122] A. Lenz and U. Nierste, *Theoretical update of $B_s - \bar{B}_s$ mixing*, *JHEP* **06** (2007) 072, [arXiv:hep-ph/0612167].

[123] M. Ciuchini, E. Franco, V. Lubicz, F. Mescia, and C. Tarantino, *Lifetime differences and CP violation parameters of neutral B mesons at the next-to-leading order in QCD*, *JHEP* **08** (2003) 031, [arXiv:hep-ph/0308029].

[124] **D0** Collaboration, V. M. Abazov *et al.*, *Search for CP violation in semileptonic B_s decays*, *arXiv:*0904.3907 [hep-ex] (2009).

[125] B. Grinstein, *Global duality in heavy flavor hadronic decays*, *Phys. Lett.* **B529** (2002) 99–104, [arXiv:hep-ph/0112323].

[126] B. Grinstein, *Global duality in heavy flavor decays in the 't Hooft model*, *Phys. Rev.* **D64** (2001) 094004, [arXiv:hep-ph/0106205].

[127] C. Berger and L. M. Sehgal, *An upper limit on CP violation in the $B_s^0 - \bar{B}_s^0$ system*, *arXiv:*1007.2996 [hep-ph] (2010).

[128] C. W. Bauer and N. D. Dunn, *Comment on new physics contributions to Γ_{12}^s*, *arXiv:*1006.1629 [hep-ph] (2010).

[129] A. Dighe, A. Kundu, and S. Nandi, *Enhanced B_s–$\bar{B}_s$ lifetime difference and anomalous like-sign dimuon charge asymmetry from new physics in $B_s \to \tau^+\tau^-$*, *arXiv:*1005.4051 [hep-ph] (2010).

[130] N. G. Deshpande, X.-G. He, and G. Valencia, *D0 Dimuon Asymmetry in $B_s - \bar{B}_s$ Mixing and Constraints on New Physics*, *arXiv:*1006.1682 [hep-ph] (2010).

[131] **D0** Collaboration, V. M. Abazov *et al.*, *Lifetime difference and CP-violating phase in the B_s^0 system*, *Phys. Rev. Lett.* **98** (2007) 121801, [arXiv:hep-ex/0701012].

[132] **CDF** Collaboration, T. Aaltonen *et al.*, *First Flavor-Tagged Determination of Bounds on Mixing- Induced CP Violation in $B_s^0 \to J/\psi\phi$ Decays*, *Phys. Rev. Lett.* **100** (2008) 161802, [arXiv:0712.2397 [hep-ex]].

[133] **D0** Collaboration, V. M. Abazov *et al.*, *Measurement of B_s^0 mixing parameters from the flavor-tagged decay $B_s^0 \to J/\psi\phi$*, *Phys. Rev. Lett.* **101** (2008) 241801, [arXiv:0802.2255 [hep-ex]].

[134] T. Feldmann, M. Jung, and T. Mannel, *Is there a non-Standard-Model contribution in non-leptonic $b \to s$ decays?*, *JHEP* **08** (2008) 066, [arXiv:0803.3729 [hep-ph]].

[135] A. J. Buras and D. Guadagnoli, *Correlations among new CP violating effects in $\Delta F = 2$ observables*, *Phys. Rev.* **D78** (2008) 033005, [arXiv:0805.3887 [hep-ph]].

[136] M. Misiak *et al.*, *The first estimate of $B(\bar{B} \to X_s\gamma)$ at $O(\alpha_s^2)$*, *Phys. Rev. Lett.* **98** (2007) 022002, [arXiv:hep-ph/0609232].

[137] M. Ciuchini, G. Degrassi, P. Gambino, and G. F. Giudice, *Next-to-leading QCD corrections to $B \to X_s\gamma$: Standard model and two-Higgs doublet model*, *Nucl. Phys.* **B527** (1998) 21–43, [arXiv:hep-ph/9710335].

[138] F. Borzumati and C. Greub, *2HDMs predictions for $\bar{B} \to X_s\gamma$ in NLO QCD*, *Phys. Rev.* **D58** (1998) 074004, [arXiv:hep-ph/9802391].

[139] P. Ciafaloni, A. Romanino, and A. Strumia, *Two-loop QCD corrections to charged-Higgs-mediated $b \to s\gamma$ decay*, *Nucl. Phys.* **B524** (1998) 361–376, [arXiv:hep-ph/9710312].

[140] M. Misiak and M. Steinhauser, *NNLO QCD corrections to the $\bar{B} \to X_s\gamma$ matrix elements using interpolation in m_c*, *Nucl. Phys.* **B764** (2007) 62–82, [arXiv:hep-ph/0609241].

[141] C. W. Bauer, Z. Ligeti, M. Luke, A. V. Manohar, and M. Trott, *Global analysis of inclusive B decays*, *Phys. Rev.* **D70** (2004) 094017, [arXiv:hep-ph/0408002].

[142] P. Gambino and M. Misiak, *Quark mass effects in $B \to X_s\gamma$*, *Nucl. Phys.* **B611** (2001) 338–366, [arXiv:hep-ph/0104034].

[143] C. W. Bauer, *Corrections to moments of the photon spectrum in the inclusive decay $B \to X_s\gamma$*, *Phys. Rev.* **D57** (1998) 5611–5619, [arXiv:hep-ph/9710513].

[144] M. Neubert, *Renormalization-group improved calculation of the $B \to X_s + \gamma$ branching ratio*, *Eur. Phys. J.* **C40** (2005) 165–186, [arXiv:hep-ph/0408179].

[145] H. E. Logan and D. MacLennan, *Charged Higgs phenomenology in the lepton-specific two Higgs doublet model*, *Phys. Rev.* **D79** (2009) 115022, [arXiv:0903.2246 [hep-ph]].

[146] H. E. Logan and D. MacLennan, *Charged Higgs phenomenology in the flipped two Higgs doublet model*, *Phys. Rev.* **D81** (2010) 075016, [arXiv:1002.4916 [hep-ph]].

[147] A. G. Akeroyd, C. H. Chen, and S. Recksiegel, *Measuring $B^\pm \to \tau^\pm\nu$ and $B_c^\pm \to \tau^\pm\nu$ at the Z peak*, *Phys. Rev.* **D77** (2008) 115018, [arXiv:0803.3517 [hep-ph]].

[148] A. G. Akeroyd and F. Mahmoudi, *Constraints on charged Higgs bosons from $D_s^\pm \to \mu^\pm\nu$ and $D_s^\pm \to \tau^\pm\nu$*, *JHEP* **04** (2009) 121, [arXiv:0902.2393 [hep-ph]].

[149] G. Barenboim, P. Paradisi, O. Vives, E. Lunghi, and W. Porod, *Light charged Higgs at the beginning of the LHC era*, *JHEP* **04** (2008) 079, [arXiv:0712.3559 [hep-ph]].

[150] R. S. Gupta and J. D. Wells, *Next Generation Higgs Bosons: Theory, Constraints and Discovery Prospects at the Large Hadron Collider*, *Phys. Rev.* **D81** (2010) 055012, [arXiv:0912.0267 [hep-ph]].

[151] Y. H. Ahn and C.-H. Chen, *New charged Higgs effects on* $\Gamma_{K_{e2}}/\Gamma_{K_{\mu 2}}$, f_{D_s} *and* $\mathcal{B}(B^+ \to \tau^+\nu)$ *in the Two-Higgs-Doublet model*, *Phys. Lett.* **B690** (2010) 57–61, [arXiv:1002.4216 [hep-ph]].

[152] A. S. Joshipura and B. P. Kodrani, *Fermion number conservation and two Higgs doublet models without tree level flavour changing neutral currents*, *arXiv:1004.3637 [hep-ph]* (2010).

[153] C. B. Braeuninger, A. Ibarra, and C. Simonetto, *Radiatively induced flavour violation in the general two- Higgs doublet model with Yukawa alignment*, *arXiv:*1005.5706 [hep-ph] (2010).

[154] A. J. Buras, M. V. Carlucci, S. Gori, and G. Isidori, *Higgs-mediated FCNCs: Natural Flavour Conservation vs. Minimal Flavour Violation*, *arXiv:*1005.5310 [hep-ph] (2010).

[155] A. J. Buras, P. H. Chankowski, J. Rosiek, and L. Slawianowska, $\Delta M_s/\Delta M_d$, $\sin 2\beta$ *and the angle* γ *in the presence of new* $\Delta F = 2$ *operators*, *Nucl. Phys.* **B619** (2001) 434–466, [arXiv:hep-ph/0107048].

[156] D. Becirevic, V. Gimenez, G. Martinelli, M. Papinutto, and J. Reyes, *B-parameters of the complete set of matrix elements of* $\Delta B = 2$ *operators from the lattice*, *JHEP* **04** (2002) 025, [arXiv:hep-lat/0110091].

[157] A. J. Buras, M. Jamin, and P. H. Weisz, *Leading and next-to-leading QCD corrections to epsilon parameter and* B^0–$\bar{B}^0$ *mixing in the presence of a heavy top quark*, *Nucl. Phys.* **B347** (1990) 491–536.

[158] S. Herrlich and U. Nierste, *The Complete* $|\Delta S| = 2$ *Hamiltonian in the Next-To- Leading Order*, *Nucl. Phys.* **B476** (1996) 27–88, [hep-ph/9604330].